1987

Application of the transient energy function method to stressed large-scale power systems

Sankaran Rajagopal
Iowa State University

INFORMATION TO USERS

While the most advanced technology has been used to photograph and reproduce this manuscript, the quality of the reproduction is heavily dependent upon the quality of the material submitted. For example:

- Manuscript pages may have indistinct print. In such cases, the best available copy has been filmed.
- Manuscripts may not always be complete. In such cases, a note will indicate that it is not possible to obtain missing pages.
- Copyrighted material may have been removed from the manuscript. In such cases, a note will indicate the deletion.

Oversize materials (e.g., maps, drawings, and charts) are photographed by sectioning the original, beginning at the upper left-hand corner and continuing from left to right in equal sections with small overlaps. Each oversize page is also filmed as one exposure and is available, for an additional charge, as a standard 35mm slide or as a 17"x 23" black and white photographic print.

Most photographs reproduce acceptably on positive microfilm or microfiche but lack the clarity on xerographic copies made from the microfilm. For an additional charge, 35mm slides of 6"x 9" black and white photographic prints are available for any photographs or illustrations that cannot be reproduced satisfactorily by xerography.

Rajagopal, Sankaran

APPLICATION OF THE TRANSIENT ENERGY FUNCTION METHOD TO STRESSED LARGE-SCALE POWER SYSTEMS

Iowa State University PH.D. 1987

Application of the transient energy function method to stressed large-scale power systems

by

Sankaran Rajagopal

A Dissertation Submitted to the
Graduate Faculty in Partial Fulfillment of the
Requirements for the Degree of
DOCTOR OF PHILOSOPHY

Major: Electrical Engineering

Approved:

Signature was redacted for privacy.

In Charge of Major Work

Signature was redacted for privacy.

For the Major Department

Signature was redacted for privacy.

For the Graduate College

Iowa State University
Ames, Iowa

1987

TABLE OF CONTENTS

CHAPTER I. INTRODUCTION

Transient Stability Assessment in Power System Operation

Transient stability studies involve analyzing whether a power system following a large disturbance will have a safe transition to an acceptable steady-state operating condition [1]. In the last two decades and in particular, after the famous blackout in Northeast U.S.A. in 1965, considerable research effort has gone into the stability investigation of power systems. At the design stage, the planner takes many contingencies into consideration to plan the location of generation, transmission system, the switch gear, and to provide operating guidelines. In subsequent operation and augmentation of the network, new considerations arise which may not have been foreseen by the planner. Hence, entirely different patterns of system behavior may be observed under actual operating conditions.

An emerging need of power system operations deals with obtaining the stability limits for various planned or forced equipment outages under changing operating conditions. For instance, these stability limits of interest can be in terms of power generation of an economic unit or power transfer across certain critical interfaces of the transmission system [2]. The system operator, given these safe limits, would take necessary actions to remain within these limits to avoid any stability crisis. Fast computation of stability limits requires a dependable analytical technique, which should be fast enough to provide answers in near real time.

The direct stability analysis based on the transient energy function (TEF) method is a potential candidate [3] to meet the requirements for real time transient stability evaluation. The avoidance of lengthy step-by-step time domain solutions and provisions for qualitative measure of the degree of system stability (namely, the energy margin) are the features that make the TEF method an attractive candidate for fast computation of stability limits. This dissertation attempts to develop the TEF method to suit the needs of the power system operations in fast computation of stability limits.

Need for Analysis of Stressed Large-scale Power Systems

In North America, the advent of extensive interconnected operation and the inability of utilities to install additional transmission capacity (due to delays, opposition and nonavailability of transmission corridors) has led to near maximum loading of transmission lines in certain regions. In many parts of the network, the stressed system conditions are created by a high level of system loading, heavy power transfers across certain transmission interfaces, or heavy loading of certain power plants for economic operation. Under these stressed conditions, the power system is vulnerable to disturbances that can affect reliability [4].

When the area of system stress encompasses most of the interconnected system, the system has to be represented in its entirety [5]. In such cases, geographically remote disturbances can have an effect upon other portions of the system. Large interconnected

systems have numerous modes of oscillations. It is not unlikely that some of the modes may be superimposed [6, Chapter 6] at some time after the start of the transient in such a way to cause increased rotor angle deviations. Moreover, it may be necessary to identify exactly the key areas that separate from the system in the extreme situations. Hence, it is necessary to represent the stressed systems in large scale for stability studies.

Even simple disturbances in stressed systems may result in complex dynamic behavior. Hence, analytical tools must be developed to deal with such situations.

Difference in Analysis Between Unstressed and Stressed Systems

In the applications of the TEF method commonly made [7, 8], the power system is usually moderately loaded, and the system is brought to instability by an increased disturbance magnitude (e.g., longer fault duration). Most of the applications are limited to demonstrating the usefulness of the method in small or medium size power systems. The critical clearing times of disturbances are used as the basis for comparing the results of the TEF method to those obtained by conventional means. The transient behavior of systems in these cases is easy to predict and the behavior is dominated by the effect of fault location and duration. The limiting conditions of interest (e.g., power flows) are usually limited by the duration of the fault and perhaps by the power generation of units close to the location of the fault.

In contrast, a stressed system may exhibit a complex dynamic behavior. The post-disturbance network of the stressed system is characterized by weak synchronizing forces [6, Chapter 3] caused by large transmission impedances. The generators away from the fault location may also separate from the system. The dynamic phenomenon can be described as follows. Following the disturbance, a small group of generators close to the fault location are severely disturbed initially. But, as the transient progresses, the weak synchronizing forces in the system dominate. When the instability occurs, it takes place as a separation of a large group of generators (including the generators severely disturbed by the fault initially) from the rest of the system. This is the so-called inter-area mode phenomenon of the stressed systems. In the extreme situations of instability, the post-disturbance network with the loss of critical transmission facility may not even be steady-state stable. The stability limited conditions of interest in operating the stressed systems (e.g., power transfer across a critical transmission interface) may be limited by the power generation levels of units away from the fault location.

The analysis of transients in a stressed system can be complex. When the first swing transient analysis is made by conventional means, the time solution must be run for a long period (2-3 seconds) to detect the system separation and the areas that separate. The analysis of inter-area mode phenomenon by the direct method based on TEF method, can also be a complex task. A host of analytical and numerical issues

are encountered and must be dealt with.

The Main Issues in the TEF Method

The direct stability analysis using the TEF method involves calculating the post-disturbance equilibrium points of the system. Among such equilibrium points, the stable equilibrium point, $\underline{\theta}^s$, and the controlling (relevant) unstable equilibrium point (UEP), $\underline{\theta}^u$, are of interest for the purpose of transient stability analysis. For a multimachine power system, the transient energy (V) is made up of two components: potential energy (PE) and kinetic energy (KE). The system transient energy, V, is evaluated with respect to the post-disturbance equilibrium conditions. Its critical value, V_{cr}, is given by the value of the potential energy at the controlling UEP, V^u, for the particular disturbance under investigation [8].

The first swing stability assessment of the system is made by computing the difference between the value of V at the end of the disturbance and V^u. Stability is maintained if $V < V^u$, or if the energy margin $\Delta V = (V^u - V) > 0$; the converse is also true. The energy margin provides a qualitative measure of the degree of system stability.

For accurate stability assessment, it is essential to account for the effect of disturbance under investigation. Identifying the group of most severely disturbed generators is the heart of the mode of disturbance (MOD) test. It was previously called the mode of instability test [9]. Identifying the correct MOD determines the accurate evaluation of the transient energy responsible for system

separation and identifies the relevant unstable equilibrium point (UEP). The UEP is an unstable steady-state solution of system equations, in which the angles of certain generators will be generally greater than $\pi/2$ (for the case where the disturbance causes the generators to accelerate). The relevant UEP is the one among many UEP solutions that may exist. Having identified the relevant UEP, it should be calculated accurately from the system equations in the post-disturbance system.

As pointed out earlier, the weak synchronizing forces in the stressed large-scale systems may lead to a large number of generators separating from the system, following a large disturbance. The determination of the mode of disturbance involves the inspection of several candidate modes provided by the analyst [9]. The accurate assessment of the critical energy, as well as the transient energy, depends primarily on the determination of MOD. It is apparently crucial to select the candidate modes properly, in order to determine the actual MOD. The number of critical generators can be very large in the stressed large-scale systems. Hence, the selection of candidate modes by the analyst is virtually not possible. It is vital to develop the TEF method to accommodate the automatic selection of candidate modes.

Further, the stress in the system results in numerical ill-conditioning of the various calculations involved in solving for the relevant UEP. Hence, it is important to select a robust numerical technique to determine the exact UEP quickly and reliably.

Review of Methods to Calculate Critical Energy and Transient Energy

In 1958, Aylett [10] formulated the energy expressions, based on intermachine motion. He explained the physical meaning of the unstable equilibrium point (UEP) by means of phase plane trajectories. The unstable equilibrium points were determined using a network analyzer for a three machine problem with the classical model [6, Chapter 2] for machines. Aylett explained how the separatrix passing through the UEP separates the stable and unstable regions of rotor angles and speeds.

The approach of formulating the system equations with respect to the system inertial center [11, 12] improved the calculation of transient energy. The inertial center formulation removes the component of system transient energy that does not contribute to instability, namely, the energy that accelerates the inertial center. Further, this inertial center formulation enables an analyst to draw an analogy between each machine of a multimachine system and the one machine - infinite bus system.

Inaccurate estimates of critical energy (V_{cr}) have often been the reason for erroneous stability assessment in the energy methods. A great deal of attention has been given by the researchers toward identification of correct critical energy levels. In essence, it involves identifying an appropriate UEP among numerous UEP solutions existing in a multimachine system.

The understanding of the effect of a major disturbance (the loss of transmission facility or generation) on the electromechanical

behavior of the system is very essential for the task of identification of relevant unstable equilibrium point (UEP). The critical energy is the potential energy level at the relevant UEP [13]. Gupta and El-Abiad [13] identified that the UEP of least potential energy or the lowest saddle of potential energy surfaces may not be near the trajectory at all, and it may lead to very conservative results. With the explanation based on the system behavior, the relevant UEP was identified as the one with minimum energy level among the UEPs close to the trajectory. The major contribution of the authors is the pragmatic approach of eliminating the UEP states that are of no relevance to a specific trajectory being investigated. But, for identification of the relevant UEP, it may not be enough to compare the energies alone at the respective UEPs near the trajectory. The effect of disturbance must be properly accounted, while comparing several UEPs, especially when there are many UEPs near the trajectory.

Kakimato et al. [14] made a significant contribution toward better understanding of critical energy and potential energy distribution in the rotor angle space. The system torque was related to the system separation, while the trajectory crosses the stable region or the boundary of the potential energy surfaces. This boundary of the potential energy is identified to be the curve that is orthogonal to the constant potential energy contours in the rotor angle space. This boundary that passes through all the UEPs was later named as the Potential Energy Boundary Surface (PEBS).

Ribbens-Pavella et al. [15] chose the approximate relevant UEP for the situation of machine K with the largest acceleration separating from the system. The machine accelerations compared were at the instant of removal of the disturbance. This selection may work well with the small systems, but is likely to give inconsistent results when several generators are disturbed in a large system. Uyemura and Matsuki [16] characterized the UEPs with the algebraic sign of eigenvalues of the matrix of Jacobian of the accelerating powers. Their critical energy calculation makes use of the approximate eigenvalues, neglecting transfer conductances. But for heavily loaded systems, the transfer conductances of the admittance matrix reduced to the internal nodes of the generators can be very large and hence, cannot be fully neglected. Bergen and Hill [17] presented a novel approach to find the critical energy for network models with the potential energy function that preserves the structure of the network. They assigned an index of vulnerability to each cutset in the network near the fault location. The vulnerability index is based on the energy of the approximate candidate UEP that corresponds to the system separation across the given cutset.

The investigators at Systems Control, Inc. (SCI) made an exhaustive attempt to develop the TEF method for practical applications in transient stability. Their attempts and the results were published in [7]. The major contributions were:

i) Approximating the effect of transfer-conductances of the network admittance matrix in the potential energy expression. This

approximation significantly improved the critical energy calculations.

2) Verifying the effect of fault location playing a vital role in the identification of the relevant UEP.

3) Developing algorithms and numerical techniques for the directions of search toward computing the relevant UEP accurately. (It should be noted that the earlier works primarily employed approximate UEPs and neglected the transfer-conductances.)

4) Suggesting faulted trajectory approximation for sustained faults.

5) Understanding and explaining of system separation using the Potential Energy Boundary Surface (PEBS) concept; formulating an instability conjecture based on this concept; and approximating the critical energy, as the energy when the trajectory of the sustained fault crosses the PEBS.

At this stage, there were still certain drawbacks in the TEF method. The direction of search for the UEP was in the direction of the machine with largest acceleration. This only accounted for the effect of disturbance, but did not take into account the effect of the post-disturbance configuration. Approximating the critical energy using the PEBS approach led to inaccurate critical energy calculations, as the PEBS, in many situations, did not have a flat potential energy profile near the UEP.

The research group at Iowa State University applied the TEF method to realistic networks for practical applications by improving the method considerably. A summary of their work is given below.

Fouad et al. [8] and Fouad and Stanton [18] validated the concept of controlling (relevant) UEP after conducting numerous simulation studies on realistic networks. The controlling UEP is the UEP closest to the trajectory of the disturbed system and it decides the first swing stability of the system. It was validated that the critical energy, for the first swing transient stability studies, will be the potential energy evaluated at the controlling UEP. They showed that all of the transient kinetic energy is not responsible for the separation of the critical generators from the rest of the system. A procedure to correct for the kinetic energy that does not correspond to the system separation was proposed, considering the gross motion of the critical generators tending to separate from the system. The kinetic energy correction removed some of the conservative nature of the transient energy calculations of the past.

Fouad et al. [8] and Fouad and Stanton [18] made a crucial observation that the generators advanced in the controlling UEP may include the generators that do not lose synchronism initially. The potential of the TEF method was identified for applications such as dynamic security assessment other than the traditional critical clearing time calculations.

The identification and the actual calculation of the controlling UEP in the absence of time solutions is a challenging task. Fouad et al. [9] evolved a criterion to identify the controlling UEP among several probable candidate UEPs provided by the analyst. The criterion provided by them accounts for two important aspects of the transient behavior

of the systems, namely, i) the effect of disturbance on various generators and ii) the energy absorbing capacity of the post-disturbance network.

Fouad and Vittal [19] and Michel et al. [20] employed the critical energies of individual machines to explain the mechanism of certain generators separating from the system. They also provided an analytical justification for the construction of domain of attraction [21, Chapter 5] or the region of stability based on individual machine energies. The transient energy functions for individual machines have been used for analyzing the output of a conventional transient stability program [22] to derive additional useful information. The output analysis is helpful, especially in reducing the number of expensive computer runs in a stability study.

Motivation for the Present Work

The varying stressed system conditions and their vulnerability to large disturbances pose a need for fast computation of system capabilities to be provided to the power system operators. Disturbances of short duration can have a large impact on the stressed system, and may result in complex dynamic behavior of the system. The rising need for faster and better analytical tools, in the operation of stressed systems, has motivated this dissertation to apply the transient energy function method to stressed large-scale systems.

In the literature reviewed so far, the TEF method has been used for the stability assessment of small or medium size power systems.

In the unstressed medium size networks, the determination of MOD is often straightforward; the transient behavior of the system is easy to analyze; obtaining the relevant UEP solution is often not complex. The TEF method has been validated in the stability assessment of unstressed medium size power networks [8].

In extending the application of the TEF method to stressed large-scale systems, a host of analytical and numerical issues, discussed earlier, arise. This dissertation specifically addresses these issues to develop the TEF method to a stage where it can be applied to the stressed large-scale systems, efficiently and reliably.

Scope of the Work

The objectives of this research endeavor are:

1) Develop a reliable scheme to automatically generate the candidate modes of disturbance and analyze them to predict the actual mode of disturbance (MOD). This scheme should not be computationally prohibitive for stressed large-scale systems in which the number of critical generators can be very large.

2) Develop a robust algorithm for solving the controlling (relevant) unstable equilibrium point (UEP) accurately. The numerical technique employed must be able to overcome the severe ill-conditioning involved in stressed systems. At the same time, the technique must be computationally efficient for problems of large sizes.

3) Understand and explain the inter-area mode of behavior of the stressed large-scale systems and its implications in the TEF method.

4) Provide justification of the UEP solution obtained in the inter-area mode cases. In these cases, there will be a shift in the MOD, i.e., the UEP will have a large number of generators advanced over and above the generators initially affected by the disturbance. When no UEP solution is obtained, verify that the post-disturbance system is steady-state unstable.

5) Conduct simulation studies and validate the schemes developed for the application of TEF method to stressed large-scale power systems. The stressed realistic power networks used were derived from a base case of the Ontario Hydro system. The initial and the post-disturbance conditions selected for the study represent highly stressed power system conditions.

CHAPTER II. MATHEMATICAL MODEL AND SIMULATION

System Equations

In this research work, the transient behavior of the multimachine system is studied using the so-called classical model [6, Chapter 2]. This model is simple enough to represent a large system, but limited to the first swing stability study. The following assumptions are made in arriving at the classical model:

1) Constant mechanical input to each generator.

2) Each generator is modeled as a constant voltage behind transient reactance.

3) Loads are represented by passive impedances.

4) Damping is negligible.

5) The motion of generator rotor coincides with the angle of the voltage behind transient reactance.

The swing equations of the machines describing the motion of the generators in the classical model are:

$$M_i\dot{\omega}_i = P_i - P_{ei}$$

$$\dot{\delta}_i = \omega_i \qquad i = 1, 2, \ldots, n \qquad (2.1)$$

where

$$P_{ei} = \sum_{\substack{j=1 \\ j\neq i}}^{n} C_{ij}\sin\delta_{ij} + D_{ij}\cos\delta_{ij}$$

$$P_i = P_{mi} - E_i^2 G_{ii} \tag{2.2}$$

where

C_{ij} = $E_i E_j B_{ij}$,

D_{ij} = $E_i E_j G_{ij}$,

δ_{ij} = $\delta_i - \delta_j$,

P_{mi} = mechanical power input,

G_{ii} = driving point conductance,

E_i = constant voltage behind transient reactance,

ω_i, δ_i = generator rotor speed and angle deviations, respectively, with respect to a synchronously rotating reference frame,

M_i = moment of inertia constant, and

$G_{ij}(B_{ij})$ = transfer-conductance (susceptance) in the admittance matrix reduced to the generator internal nodes, for the post-disturbance network.

The system equations are then transformed into the inertial center reference frame. The primary reason for this transformation is to conveniently remove the kinetic energy associated with the acceleration of the inertial center of the system [7, 8]. Further, this inertial center formulation provides a better physical insight into the

transient stability problem formulation. The position and speed of the center of inertia (COI) are given by:

$$\delta_o = \frac{1}{M_T} \sum_{i=1}^{n} M_i \delta_i$$

$$\omega_o = \dot{\delta}_o = \frac{1}{M_T} \sum_{i=1}^{n} M_i \omega_i \qquad (2.3)$$

where

$$M_T = \sum_{i=1}^{n} M_i \quad .$$

The generator angles and speeds with respect to the COI are:

$$\theta_i = \delta_i - \delta_o$$

$$i = 1, 2, \ldots, n \qquad (2.4)$$

$$\tilde{\omega}_i = \omega_i - \omega_o$$

It can be noticed that $\underline{\theta}$, $\underline{\tilde{\omega}}$ always satisfy the constraints of the inertial center reference frame, namely,

$$\sum_{i=1}^{n} M_i \theta_i = 0 \ , \qquad \sum_{i=1}^{n} M_i \tilde{\omega}_i = 0 \quad . \qquad (2.5)$$

In the inertial center reference frame, the equations of motion become

$$M_i\dot{\tilde{\omega}}_i = P_i - P_{ei} - \frac{M_i}{M_T} P_{COI} = f_i$$

$$\dot{\theta}_i = \tilde{\omega}_i \qquad i=1, 2, \ldots, n \tag{2.6}$$

where

$$P_{COI} = \sum_{i=1}^{n} P_i - P_{ei} \quad .$$

Equilibrium Points

The transient energy function method requires the calculation of the equilibrium points of the post-disturbance system for stability assessment. The equilibrium points of the system are the points where the right-hand side of the swing equations (2.6) become zero. Among these equilibria, the stable equilibrium point, $\underline{\theta}^s$, and the controlling unstable equilibrium point, $\underline{\theta}^u$, are of interest for the purpose of stability assessment as explained in Chapter I.

The stable equilibrium point, $\underline{\theta}^s$, will have all the generator angles less than $\pi/2$. The calculation of $\underline{\theta}^s$ is rather straightforward, as it represents the unique post-disturbance steady-state operating condition. The unstable equilibrium points can be as many as a theoretical maximum of $2^{n-1} - 1$ for a n-machine system [13]. The controlling UEP ($\underline{\theta}^u$) is the unstable equilibrium point relevant to the disturbance under the investigation. The controlling UEP ($\underline{\theta}^u$) represents the unstable equilibrium point of the system, in which the angles of a certain group of generators are advanced (generally, greater than $\pi/2$ in the case

where the disturbance causes the generators to accelerate). The determination of the mode of disturbance, explained in Chapter I, identifies the group of generators whose angles will be advanced in the controlling UEP. The efficiency of the TEF method, to a large extent, depends upon the accurate identification and calculation of the controlling UEP.

Energy Expressions

The transient energy is evaluated with respect to the post-disturbance stable operating conditions. The system transient energy, V, comprises two primary components, namely, the kinetic energy and the potential energy.

$$V = KE + PE \quad . \tag{2.7}$$

The potential energy of the system at any point is given by

$$PE = -\sum_{i=1}^{n} P_i(\theta_i - \theta_i^s) - \sum_{i=1}^{n-1}\sum_{j=i+1}^{n} [C_{ij}(\cos\theta_{ij} - \cos\theta_{ij}^s) - \int_{\theta_i^s+\theta_j^s}^{\theta_i+\theta_j} D_{ij}\sin\theta_{ij}\, d(\theta_i + \theta_j)] \tag{2.8}$$

where

$$\theta_{ij} = \theta_i - \theta_j \quad .$$

The potential energy is comprised of three components. In the potential energy expression (Eq. 2.8), the first term is the position energy, the second term is the magnetic energy, and the third term is the dissipation energy. The dissipation energy is the energy dissipated in the network transfer-conductances. The dissipation energy term is the path dependent integral, which the direct method attempts to avoid in the first place. The path dependent integral term is, hence, approximated as suggested by Athay et al. [7] in this investigation:

$$I_{ij} = D_{ij} \frac{\theta_i + \theta_j - \theta_i^s - \theta_j^s}{\theta_{ij} - \theta_{ij}^s} (\sin\theta_{ij} - \sin\theta_{ij}^s) \quad . \qquad (2.9)$$

Kinetic Energy Correction

The transient kinetic energy responsible for the separation of the critical generators from the rest of the system is that associated with the gross motion of the critical generators [8, 18]. The remaining portion of the kinetic energy need not be absorbed by the network for the stability to be maintained.

Essentially, the disturbance splits the generators of the system into two groups: the critical machines and the rest of the generators. Their inertial centers have inertia constants and angular speeds M_{cr}, $\tilde{\omega}_{cr}$ and M_{sys}, $\tilde{\omega}_{sys}$, respectively. The gross motion of these two groups approximates that of a two-machine system.

Without loss of generality, say the first k machines are tending to separate from the system, as identified by the mode of disturbance

test. The kinetic energy causing the separation of the two groups is the same as that of an equivalent one machine - infinite bus system having inertia constant M_{eq} and angular speed $\tilde{\omega}_{eq}$ given by:

$$M_{eq} = \frac{M_{cr} \cdot M_{sys}}{M_{cr} + M_{sys}}$$

$$\tilde{\omega}_{eq} = (\tilde{\omega}_{cr} - \tilde{\omega}_{sys}) \qquad (2.10)$$

where

$$M_{cr} = \sum_{i=1}^{k} M_i \,, \qquad M_{sys} = \sum_{j=k+1}^{n} M_j$$

$$\tilde{\omega}_{cr} = \frac{\sum_{i=1}^{k} M_i \tilde{\omega}_i}{M_{cr}} \,, \qquad \tilde{\omega}_{sys} = \frac{\sum_{j=k+1}^{n} M_j \tilde{\omega}_j}{M_{sys}} \,.$$

The kinetic energy that tends to split the system into two groups is denoted as the corrected kinetic energy and is given by

$$KE_{(corr)} = 1/2 \; M_{eq} \; (\tilde{\omega}_{eq})^2 \,. \qquad (2.11)$$

Energy Margin

The critical value of the transient energy is the energy absorbing capacity of the post-disturbance network, for the disturbance under investigation. The critical energy is given by the value of the potential energy at the controlling UEP [8] denoted as V^u. The critical

energy, V^u, can be obtained by evaluating Eq. (2.8) at $\underline{\theta} = \theta^u$, with the integral term approximated by Eq. (2.9).

The first swing stability assessment of the system is made by computing the difference between the value of V at the end of the disturbance and V^u. If $V < V^u$, the stability is maintained, or if the energy margin $\Delta V = V^u - V > 0$; the converse is also true. The energy margin provides a qualitative measure of the degree of system stability. The energy margin is mathematically expressed as

$$\Delta V = V^u - V|_{\underline{\theta}^{c\ell},\ \underline{\tilde{\omega}}^{c\ell}} \tag{2.12}$$

where $\underline{\theta}^{c\ell}$ and $\underline{\tilde{\omega}}^{c\ell}$ are the rotor angles and speeds at the end of the disturbance. Equation (2.12) can further be simplified as

$$\Delta V = [\Delta V_{PE} - KE_{(corr)} \text{ at the end of disturbance}] \tag{2.13}$$

where

$$\Delta V_{PE} = PE \Big|_{\underline{\theta}^{c\ell}}^{\underline{\theta}^u} . \tag{2.14}$$

CHAPTER III. DETERMINATION OF MODE OF DISTURBANCE

For a given unstable equilibrium point (UEP), certain rotor angles are more advanced than the others (generally > $\pi/2$ for the case where the disturbance accelerates the machines). These represent the angles of the most disturbed generators. This group of machines determines the level of critical energy, V_{cr}. The mode of disturbance (MOD) is a terminology for characterizing the UEP. The UEP of interest for a given disturbance is known as the controlling UEP. It can be described by a certain group of machines severely affected by the disturbance; they include, but are not necessarily restricted to the machines initially losing synchronism in the post-disturbance network [18]. The group of machines characterizing the controlling UEP is referred to as the MOD for a given disturbance and a specific post-disturbance network.

Knowledge of the MOD is essential to arrive at the mathematical basis, such as bounds and directions of search necessary to distinguish the controlling UEP from the other UEPs in the rotor angle space. Further, the MOD information for a given disturbance determines the kinetic energy that tends to split the system at the end of the disturbance period into two groups of generators pulling away from each other. This is referred to as kinetic energy correction in Chapter II. It is essential to determine the MOD correctly for accurate stability assessment.

The analytical issues involved in the determination of MOD will be discussed in this chapter. A procedure for automating the determination

of MOD is provided.

Concept of Controlling Unstable Equilibrium Point

As pointed out in Chapters I and II, the post-disturbance system has many unstable equilibrium points. The physical meaning of the UEPs can be explained with the aid of potential energy (PE) contours in the rotor angle space. Figure 3.1 (reproduced from Reference [7]) shows the PE contours in the rotor angle space of a three-machine system with negligible transfer-conductances. The post-disturbance equilibrium, $\underline{\theta}^s$, is uniquely defined and is situated at the bottom of the bowl-shaped surface of Figure 3.1. The ridge of the PE contours, shown as a dashed line in Figure 3.1, is the potential energy boundary surface (PEBS) [7, 14]. This ridge has several saddles which are the UEPs connected by the PEBS.

The PE surfaces have higher ridges in some segments than others. Hence, the amount of rotor motion (and the corresponding energy absorbed) required to reach instability will vary from one trajectory to another. Thus, the faulted trajectory is analogous to a particle climbing up the potential energy hills around the valley. The critical energy or the capacity of the network to absorb the initial excess transient energy will vary, depending on which segment of the PE surface the trajectory moves in.

For first swing transient stability assessment, the UEP closest to the trajectory of the post-disturbance system is the one that decides the transient stability. This UEP is called the controlling UEP for

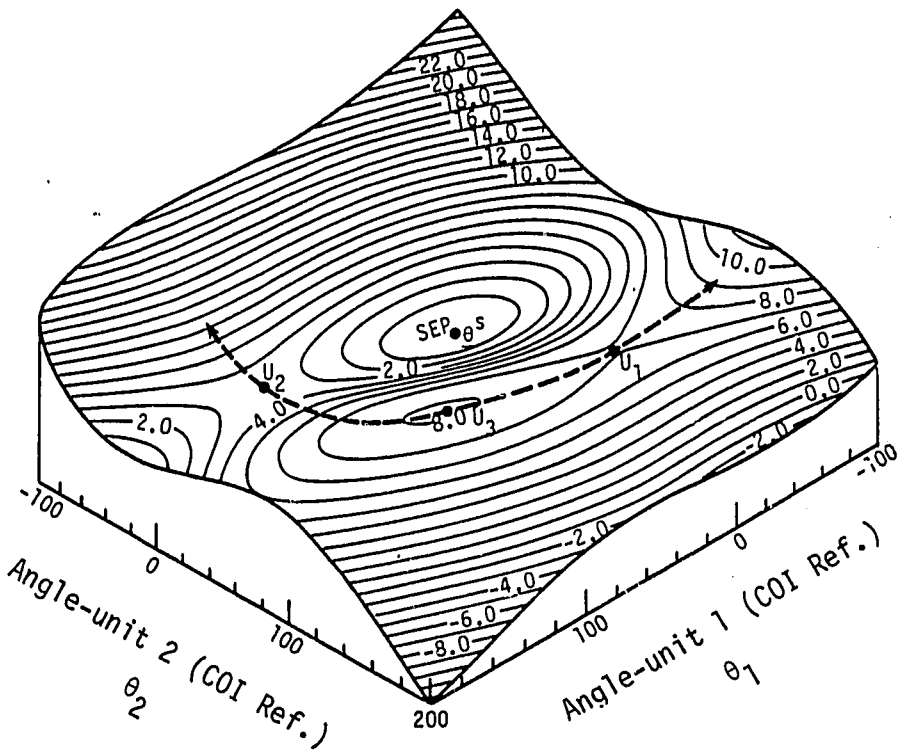

Figure 3.1. Equi-potential energy surfaces (solid lines) and the potential energy boundary surface (dashed line) for three-machine system (reproduced from Reference [7])

this trajectory [18]. The critical transient energy is the value of the potential energy at this controlling UEP for the particular disturbance under investigation. As the number of generators in the system becomes larger, the identification of the controlling UEP becomes a challenging task. Several UEPs can be close to the trajectory in a large system, especially when many generators are disturbed. Hence, accurate and efficient determination of the MOD is essential for correct transient stability assessment.

Mode of Disturbance Test

When the generators of a multimachine power system are subjected to a disturbance, their equilibrium is disturbed. During the ensuing transient, the more severely disturbed generators may or may not lose synchronism, depending on whether the potential energy absorbing capacity of the post-disturbance network is adequate to convert the transient kinetic energy of the system at the end of the disturbance into potential energy. Fouad et al. [9] present a criterion for identifying the controlling UEP among several candidates. Each candidate UEP is associated with a certain MOD. If a UEP has machines $(m_1, m_2, \ldots, m_m)$ advanced (generally, angle $> \pi/2$ for the situation where the disturbance causes these generators to accelerate), the corresponding MOD is said to be $(m_1, m_2, \ldots, m_m)$. For a given disturbance, the MOD test accounts for the following two important aspects of the transient phenomena:

1) the effect of disturbance on various generators, and

2) the energy absorbing capacity of the post-disturbance network.

The relative degree of stress to the various groupings of severely disturbed generators, associated with the corresponding UEPs, is reliably indicated by the normalized potential energy margin $\Delta V_{PE}|_n$ [19]. Each candidate UEP is assigned an index of severity, $\Delta V_{PE}|_n$ obtained by normalizing ΔV_{PE} (Eq. 2.14) with the kinetic energy (corrected) for the corresponding MOD. The criterion validated by Fouad et al. [9] proposes that the controlling UEP is the UEP with the smallest value of $\Delta V_{PE}|_n$ at the end of the disturbance period. In order to perform this MOD test, it is sufficient to have approximate UEPs pertaining to the list of candidate modes [9]. It will be computationally prohibitive to calculate all the candidate UEPs, especially for systems of large sizes.

The criterion developed by Fouad et al. [9] identifies the controlling UEP among several candidate UEPs. The analytical issue to be addressed now is the selection of candidate UEPs or modes, especially for situations involving complex dynamics in stressed large-scale systems.

Complexity in Selection of Candidate Modes of Disturbance

In the application of the TEF method validated so far in direct-stability assessment, the power networks used were of small to medium size unstressed systems. In such situations, the transient behavior of the system is often easy to predict; very few generators are found to

be severely disturbed by the large disturbance under investigation. The candidate modes of disturbance are normally selected by inspection of the system and the location of the disturbance, along with some engineering judgement. In medium size unstressed systems, only a few generators are severely disturbed at the end of the disturbance period and in the ensuing transient. Subsequently, the number of combinations of the generator groupings within these critical generators is fewer; the selection of these candidate modes is rather simple and straightforward for an experienced power system analyst.

In stressed large-scale systems, a large number of generators may separate from the rest of the system in situations involving the inter-area mode phenomenon. This phenomenon, pointed out in Chapter I, will be discussed in detail in Chapter V. As the number of critical generators is large in such situations, an analyst is left with the task of selecting and inspecting a large number of candidate groupings of these critical generators. The identification of the controlling UEP is a very crucial part of the stability assessment, as it determines the appropriate critical energy level. There is an obvious need to automate the selection of candidate modes, for improving the reliability of the TEF method for practical applications in stressed large-scale systems.

An ideal, but impractical list of candidates will be selecting all $2^{n-1}-1$ of theoretically possible combinations of modes in a systematic way. Emphasis must be given in eliminating most of the inappropriate modes or UEP states. For instance, all the combinations

of generators involving machines that are far away from the fault location can be screened right away. The final list of candidates must be narrowed down to a very few in order that the MOD test suggested by Fouad et al. [9] be computationally efficient. With the understanding of the effect of the major disturbance and the loss of the transmission facility on the electromechanical behavior of the system, the list of candidate modes must be selected efficiently.

Scheme for Automating Mode of Disturbance Determination

A systematic procedure for generating the correct mode of disturbance has been developed in this research work. The MOD determination procedure involves the following major steps:

Step A: Rank the machines by characterizing the severity of disturbance on various machines at the instant of removal of disturbance, $t_{c\ell}$, based on their KE and accelerations. The kinetic energy of each group of machines provides a measure of the severity of the disturbance. Making use of the ranking of machines, identify the generator groupings which are most seriously affected by the disturbance. These groupings are the list of candidate modes of disturbance, narrowed down for a close examination.

Step B: Each of these candidate MODs has a corresponding portion of kinetic energy at $t_{c\ell}$ that tends to split this particular group of machines from the rest of the system. This value of KE was termed as $KE_{(corr)}$ in Chapter II. To investigate the critical energy levels represented by these candidates, an approximate UEP is computed

for each of these candidates. For each candidate mode, the ability of the post-disturbance network to convert the corresponding corrected kinetic energy is examined.

The procedure followed in the above two steps is outlined below.

The first step (A) involves the following:

A-1) a) Obtain a list of machines ranked in the descending order of kinetic energy at $t_{c\ell}$, i.e., based on the quantities $M_i\tilde{\omega}^2_{c\ell i}$, where $\tilde{\omega}_{c\ell i}$ is the speed (w.r.t. COI) of machine i at $t_{c\ell}$.

b) Obtain a second list of machines, ranked in the descending order of acceleration at $t_{c\ell}$, i.e., based on the quantities $f(\theta)_{c\ell i}/M_i$, where $f(\theta)_{c\ell i}$ is the accelerating power (w.r.t. COI) of machine i at $t_{c\ell}$.

c) The machines that belong to the same power station are grouped together in a list.

d) A final list of key machines of interest is generated as follows:

M/Cs appearing in both the $M\tilde{\omega}^2_{c\ell}$ and $f(\theta)_{c\ell}/M$ lists.
M/Cs appearing in $M\tilde{\omega}^2_{c\ell}$, but not in $f(\theta)_{c\ell}/M$ list.
M/Cs appearing in $f(\theta)_{c\ell}/M$ list, but not in $M\tilde{\omega}^2_{c\ell}$ list.

This list characterizes the effect of the disturbance on the various machines. The machine on the top of the list will be most affected and at the bottom of the list, least affected.

A-2) From the bottom of the list, head towards the top of the list dropping one machine (or all the machines at the same power station) at a time. For each such case, calculate the corrected kinetic energy, $KE_{(corr)}$, at t_{cl}.

A-3) Sort and obtain a list of modes, whose $KE_{(corr)}$ is within a certain fraction of the maximum $KE_{(corr)}$, and corresponding $KE_{(corr)}$ in descending order. This provides the grouping of generators ranked according to the effect of the disturbance.

The second step (B) consists of the following:

B-1) For each of the modes of disturbance at the top of the ranked $KE_{(corr)}$ list, obtain ΔV_{PE} at the ray point (refer to Chapter IV for construction of the ray point). The MOD_k that has the least value of $\Delta V_{PE}/KE_{(corr)}$ will be the relevant MOD [9].

B-2) Use the appropriate ray point of MOD_k as the starting point for the UEP solution in order to accurately compute the controlling UEP for the given disturbance.

The details of the computer program 'MOD' of the above-cited scheme are provided in Appendix A. The ray point of MOD_k of step B-2 above is a good approximation of the controlling UEP in terms of PE value it represents. Accurate calculation of the controlling UEP will be

discussed in Chapter IV. The results obtained using this scheme for the determination of MOD will be discussed in Chapter VII.

CHAPTER IV. UNSTABLE EQUILIBRIUM POINT SOLUTION

As discussed earlier in Chapter II, the equilibrium points are the solutions in rotor angle space satisfying the condition that the right-hand side of the swing equations (2.6) are zero. Among them, the stable equilibrium point (SEP) and the controlling unstable equilibrium point (UEP) are of interest for the purpose of stability assessment. Obtaining the SEP solution is rather straightforward, as it represents the unique post-disturbance steady-state operating condition with all the rotor angles less than $\pi/2$. The controlling UEP ($\underline{\theta}^u$) is the unstable equilibrium point of the post-disturbance system in which the angles of certain group of generators are advanced (generally $> \pi/2$, for the situation where the disturbance causes the generators to accelerate). The controlling UEP is the UEP relevant to the disturbance under investigation. Since the controlling UEP represents the critical energy level for the stability assessment, it is crucial to compute it accurately.

The determination of mode of disturbance (MOD), dealt with in Chapter III, characterizes the UEP of interest by identifying which machines will have advanced angles (i.e., $> \pi/2$). This chapter mainly deals with the computational aspects involved in finding the controlling UEP. In extending the application of the transient energy function (TEF) method to stressed large-scale systems, the following issues must be dealt with:

1) Obtain a good starting point or bound for the UEP of interest

and

2) Develop a safe-guarded robust numerical technique, in order to efficiently achieve a reliable convergence to the UEP of interest.

This chapter addresses the above cited issues and the attempts that were made to solve them.

Starting Points for Unstable Equilibrium Points

For any iterative numerical technique selected for UEP solution, the reliable convergence depends on the starting point or the seed value of rotor angles. Selection of a poor starting point may increase the computational burden, and in the worst case, may lead to a wrong UEP solution. Proper attention must be given to the selection of a starting point.

For each UEP, there is a region of convergence in the rotor angle space [23, 24]. The UEP of interest lies in the proximity of the corner point of a polytope. The corner point is computed very easily from the knowledge of the post-disturbance SEP and the MOD characterizing the UEP of interest. If the MOD includes machines $(m_1, m_2, \ldots, m_m)$, the corner point is defined as

$$\begin{aligned} \theta_i &= \theta_i^s \qquad \text{for } i \neq m_k \qquad i,j = 1, 2, \ldots, n \\ \theta_j &= \pi - \theta_j^s \qquad \text{for } j = m_k \qquad k = 1, 2, \ldots, m \,. \end{aligned} \tag{4.1}$$

It should be noted that the corner point does not satisfy the COI constraint of $\sum_{i=1}^{n} M_i\theta_i = 0$ of Eq. (2.5) in the inertial center reference

frame formulation. The inertial center has advanced from its position at $\underline{\theta}^s$ to that at $\underline{\theta}^u$. It will hence, be appropriate to correct the corner point to account for the motion of inertial center, as it moves toward the UEP.

The procedure to obtain the corrected corner point is as follows:

Let the MOD be $(m_1, m_2, \ldots, m_m)$. In this case, these machines referred to as group I, separate from the rest of the machines, say group II.

1) Obtain the center of the two groups of machines at $\underline{\theta}^s$:

$$\theta_I^s = \sum_{i\epsilon I} M_i\theta_i^s/M_I$$

$$\theta_{II}^s = \sum_{j\epsilon II} M_j\theta_j^s/M_{II} \qquad (4.2)$$

where $M_I = \sum_{i\epsilon I} M_i$,

M_i = inertia of machine i,

$M_{II} = \sum_{j\epsilon II} M_j$, and

$M_T = M_I + M_{II}$.

2) The difference in inertial positions, $\theta_I^s - \theta_{II}^s = \bar{\theta}$, at $\underline{\theta}^s$ will move to $\theta_I^u - \theta_{II}^u = \pi - \bar{\theta}$ at $\underline{\theta}^u$, in the one machine - infinite bus sense. The center of inertia of this one machine - infinite bus system has advanced by $(\pi-\bar{\theta}) - \bar{\theta}$ $= \pi - 2\bar{\theta}$ between $\underline{\theta}^s$ and $\underline{\theta}^u$.

3) The corrected corner point ($\underline{\hat{\theta}}^u$) is obtained as follows, satisfying the COI constraint:

$$\hat{\theta}_i^u = \theta_i^s + \frac{M_{II}}{M_T}(\pi - 2\bar{\theta}) \qquad \text{for } i \in I$$

$$\hat{\theta}_j^u = \theta_j^s - \frac{M_I}{M_T}(\pi - 2\bar{\theta}) \qquad \text{for } j \in II \,. \tag{4.3}$$

Further improvement of this corrected corner point ($\underline{\hat{\theta}}^u$) can be obtained using the concept of the potential energy boundary surface (PEBS) from the literature [7, 14]. In the $\underline{\theta}$ space, a ray from $\underline{\theta}^s$ to $\underline{\hat{\theta}}^u$ is formed, as shown in Figure 4.1. The point $\underline{\theta}^{ray}$ indicated in this figure is the point where the potential energy (PE) reaches a relative maximum along this ray.

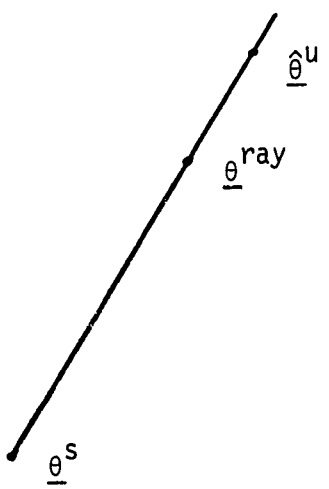

Figure 4.1. Maximum potential energy point on ray from $\underline{\theta}^s$ to $\underline{\hat{\theta}}^u$

Any point on the ray emanating from $\underline{\theta}^s$ and passing through $\hat{\underline{\theta}}^u$ can be denoted as:

$$\underline{\theta} = \underline{\theta}^s + \alpha \, \Delta\underline{\theta} \tag{4.4}$$

where $\alpha \geq 0$ and $\Delta\underline{\theta} = \hat{\underline{\theta}}^u - \underline{\theta}^s$. Let

$$\underline{f}(\underline{\theta}) = \text{vector of accelerating powers as in Eq. (2.6).} \tag{4.5}$$

Along this ray, the potential energy varies only with the scalar α. Let the value of α, where the PE reaches the first relative maximum, be α^* and the corresponding $\underline{\theta}$ will be:

$$\underline{\theta}^{ray} = \underline{\theta}^s + \alpha^* \, \Delta\underline{\theta} \quad . \tag{4.6}$$

The point $\underline{\theta}^{ray}$ will be situated at the PEBS, which is the surface of all the points of $\underline{\theta}$ where the PE assumes a relative maximum value. The PEBS is characterized by [7] all the points $\underline{\theta}$, where $\underline{f}^T(\underline{\theta}) \cdot (\underline{\theta} - \underline{\theta}^s) = 0$. Hence, a way to compute α^* will be to iterate using a one-dimensional minimization approach [25, 26] to find the α where

$$\frac{d(\text{PE along ray})}{d\alpha}\Big|_{\alpha=\alpha^*} = -\sum_{i=1}^{n} f_i(\underline{\theta} + \alpha \, \Delta\underline{\theta}) \cdot \Delta\theta_i \Big|_{\alpha=\alpha^*} = 0 \quad . \tag{4.7}$$

The value of α^* will be the least positive value α (correspondingly, the first relative maximum of PE along the ray starting from $\underline{\theta}^s$) for which, expression of Eq. (4.7) is zero [7].

Construction of the ray point ($\underline{\theta}^{ray}$) provides a computationally inexpensive method to get close to the UEP of interest. In terms of the value of PE it represents, $\underline{\theta}^{ray}$ will be close to that of the UEP being sought. In this research investigation, $\underline{\theta}^{ray}$ is used as an approximate UEP in the following situations:

1) For a given candidate MOD, obtain the ray point by using the procedure described earlier. Use this ray point, as the approximate UEP pertaining to the given candidate MOD. The scheme for the determination of MOD, given in Chapter III, makes use of this ray point as a candidate UEP.

2) For accurately solving the UEP of interest, use the corresponding ray point as the starting point or the seed value required in any iterative numerical technique or algorithm. An accurate calculation of the controlling UEP is quite necessary for a correct estimate of the critical energy.

Methods for Unstable Equilibrium Point Solution

Problems in obtaining UEPs

There are two major sets of problems in obtaining the UEP solution, originating from:

1) System size. These problems relate to the following:

- solution speed

- convergence to a solution
- obtaining the correct solution.

2) System operating conditions. These conditions lead to difficulties in the following:

- convergence to a solution
- convergence to the correct solution.

Obtaining a wrong UEP solution would have the consequence of obtaining a wrong value of critical energy for stability assessment. It is essential to select a robust numerical technique to obtain the correct UEP solution, especially in stressed systems. In the case of stressed systems, a severe numerical ill-conditioning was observed owing to the system operating conditions. The details of the cause of ill-conditioning will be discussed in Chapter V.

It was identified in this investigation that the selection of a robust numerical technique must be based on the following aspects:

1) Reliability - in terms of convergence to the UEP of interest.

2) Speed - in terms of the CPU time taken to obtain the right UEP solution.

Approaches

The following approaches can be found in the literature to solve the system of nonlinear algebraic equations of (4.5) for equilibrium points.

1) The direct solution approach. The swing equation (4.5) is directly solved for the solution, using an iterative technique. The

Newton-Raphson (NR) method has been previously used for a three-machine system of equations by Uyemura and Matsuki [16]. Athay et al. [7] observed that the NR method was slow and divergent in a few cases. When there is no numerical ill-conditioning, the NR method will converge rapidly. El-Abiad and Nagappan [27] used the method of steepest-descent to calculate the UEPs. This method is known to be very slow in convergence [25], near the solution, even for a small system of nonlinear equations.

2) Indirect solution approach. In this case, the solution technique is formulated as a 'nonlinear least-squares unconstrained minimization' problem. The objective function to be minimized is given by

$$F = \sum_{i=1}^{n} f_i^2 \tag{4.8}$$

where f_i is defined in Eq. (4.5). The Davidon-Fletcher-Powell (DFP) method, a quasi-Newton type technique, was used by Athay et al. [7] to determine the equilibrium points for a system of 20-generators. The DFP method is a robust technique, but is inefficient for systems of large size.

The methods discussed so far, NR, steepest descent and the DFP method, involve the computation of only the first derivatives explicitly. Before selecting a robust and efficient technique, it may be worthwhile to identify the effect of numerical ill-conditioning in obtaining the UEP solutions.

Numerical Ill-conditioning

A severe numerical ill-conditioning is encountered in obtaining the UEP solution when the network is heavily stressed. The stressed systems are large power networks operated close to their stability limits. The stress contributes to irregularities in the potential energy surface near the UEP. This, in turn, causes the numerical ill-condition that can significantly affect the performance of the UEP solution techniques.

As an illustrative example, consider the linear system of equation of the form $\underline{A}\underline{X} = \underline{B}$. The exact solution exists if and only if $\underline{A}$ is nonsingular. Consider an example where

$$\underline{A} = \begin{bmatrix} 0.55 & 0.423 \\ 0.484 & 0.372 \end{bmatrix} , \quad \underline{B} = (0.127, 0.112)^T, \quad \underline{X} = \underline{A}^{-1}\underline{B} \qquad (4.9)$$

where the exact solution $\underline{X} = (1, -1)^T$. If $\underline{B}$ is perturbed such that $\underline{B} + \Delta\underline{B} = (0.12707, 0.11228)$, for $\Delta\underline{B} = (0.0007, 0.00028)^T$, the exact solution becomes $\underline{X} + \Delta\underline{X} = (1.7, -1.91)^T$, with $\Delta\underline{X} = (0.7, -0.91)^T$. Using an infinity norm (the largest absolute row sum), it can be observed that the relative change in $\underline{X}$ will be $||\Delta\underline{X}||/||\underline{X}|| = 0.91$, which is much larger than the relative change in $\underline{B}$ vector, $||\Delta\underline{B}||/||B|| = 0.0022$.

Similarly, if $\underline{A}$ is perturbed in (2,1) position in the third decimal, so that

$$\underline{A} + \Delta\underline{A} = \begin{bmatrix} 0.55 & 0.423 \\ 0.483 & 0.372 \end{bmatrix} ,$$

then, the solution to the perturbed system of $(\underline{A} + \Delta\underline{A})(\underline{X} + \Delta\underline{X}) = \underline{B}$ will be $\underline{X} + \Delta\underline{X} = (-0.4535, 0.8899)^T$. The relative change in $\underline{X}$ is much larger than the relative change in $\underline{A}$. The matrix $\underline{A}$ is ill-conditioned, with a condition number of $||\underline{A}||/||\underline{A}^{-1}|| = 0.973 \times 7834 = 7622$.

It should be emphasized that the perturbation analysis concerns the exact solution of a linear system and is therefore, an inherent characteristic of the mathematical problem [25]. With regard to the implications of the ill-conditioning, the $\underline{A}$ matrix of the illustrative example is analogous to the Jacobian of the swing equation vector. In the NR method, the updating procedure for the UEP solution is:

$$\underline{\theta}^{(k+1)} = \underline{\theta}^{(k)} + \alpha^{(k)} \, (\Delta\underline{\theta})^{(k)} \tag{4.10}$$

in iteration k, where

$$\Delta\underline{\theta} = - \underline{J}^{-1} \, \underline{f}$$

$$J = [\frac{df_i}{d\theta_j}] = \text{Jacobian}$$

$$\alpha = \text{step length.}$$

The ill-conditioned Jacobian matrix may lead to the following problems in a first derivative method like the NR method:

1) Divergence or convergence to a wrong UEP solution, or
2) No progress in the solution due to the repeated values of

$\alpha = 0$, controlled by the step length [26] calculation.

In certain cases of ill-conditioning, the scaling of variables in the NR method can enhance the reliability of the method. The scaling of the variables is helpful, especially in the situation where the method is found to be very slow in progress.

Consider an illustrative example:

$$h(x_1, x_2) = x_1^2 + 10^4 x_2^2 \quad . \tag{4.11}$$

The function $h(x_1, x_2)$ has sensitivity to variations in x_1 equal to about 10^4 times its sensitivity to x_2 variations, when x_1 and x_2 have the same order of magnitude. These unbalanced gradients may pose convergence difficulties in the first derivative based iterative methods, such as NR method and steepest descent. The variable transformation $x_2' = 100\ x_2$ would lead to $h = x_1^2 + x'^2_2$, which represents a much easier functional surface to iterate on, as shown in Figure 4.2. The general updating of the solution in the scaled-Newton-Raphson method will be

$$\underline{\theta}^{(k+1)} = \underline{\theta}^{(k)} + \underline{T}^{(k)}\ \underline{\Delta\theta}^{(k)} \tag{4.12}$$

where $\underline{T}^{(k)}$ is the diagonal matrix of transformation at k^{th} iteration. The performance of the SNR method, developed elsewhere, is quite satisfactory to calculate the SEPs in all cases and the UEPs in the case of the unstressed large-scale systems. But, in the case of the

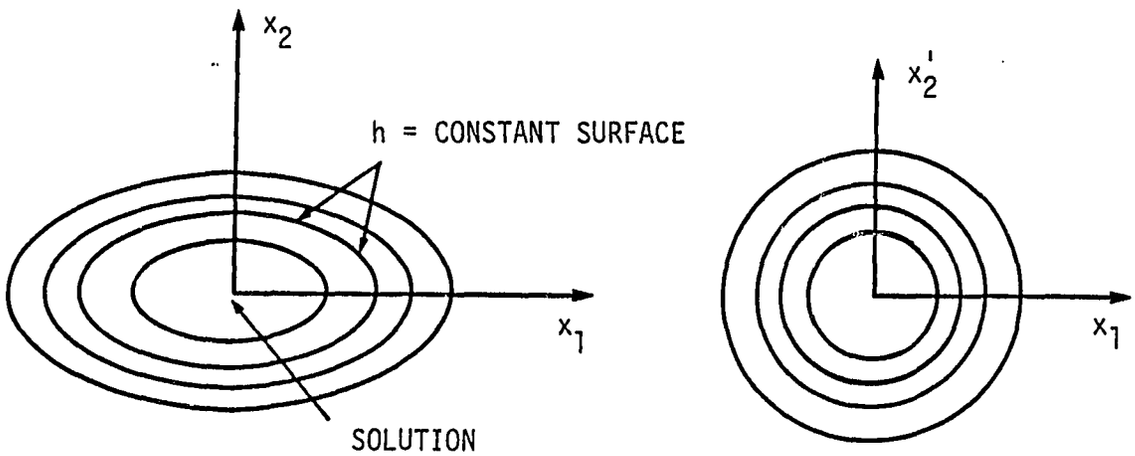

Figure 4.2. Effect of variable transformation

stressed, ill-conditioned systems, the SNR method diverged during UEP solutions.

The DFP method was found to be robust. But it was observed to be very slow in UEP solutions of stressed large-scale systems and did not converge in some ill-conditioned cases. The DFP algorithm is a quasi-Newton method [25, 26]. It is based on the theory that an approximation to the curvature of a nonlinear function can be computed without explicitly forming the Hessian [$\nabla^2 F$] matrix.

After a careful search of the various methods available to solve the nonlinear least-squares minimization and taking into consideration the system sizes dealt with, the corrected Gauss-Newton method was selected in this research investigation.

Corrected Gauss-Newton Method

The corrected Gauss-Newton (CGN) method is a modification to the Gauss-Newton method of solving the nonlinear least-squares type problems. This method [28] seeks to avoid the deficiencies in the Gauss-Newton method by improving, when necessary, the Hessian approximation by specifically including or approximating some of the neglected terms. The swing equations $\underline{f}(\underline{\theta})$ of Eq. (4.5) have the second derivatives in a closed form (see Appendix B). The CGN method makes use of the second derivatives, only when the algorithm does not make a satisfactory progress. The heart of the method lies in the singular value decomposition of the Jacobian matrix to detect the ill-conditioning of Jacobian [25]. The ratio of the largest to the

smallest singular value is used as a measure of ill-conditioning.

In each iteration of the solution procedure, the algorithm has the provision for checking the singular values of the Jacobian. Under normal circumstances, the first derivatives are only computed. If the ill-conditioning is detected, the solution space is split into two subspaces, one associated with the large singular values and the other associated with the small singular values. The first derivative information is used in the former solution space. The first and second derivatives are used in the latter solution space. With the result, the diverging effect due to inverting the small singular values of the Jacobian is avoided. Thus, the method is safeguarded against divergence due to the numerical ill-conditioning. The basic algorithm of the CGN method is summarized as follows.

1) Select $\underline{x}^{(o)}$; calculate $f_i^{(o)}$ i=1,2,...,n and $\underline{J}^{(o)} = [\partial \underline{f}/\partial \underline{x}] \Big|_{\underline{x} = \underline{x}^o}$ and $\underline{g}^{(o)} = 2\, \underline{J}^{(o)T} \underline{f}^{(o)}$.

2) If $\underline{x}^{(k)}$ is an adequate approximation to the stationary point, the algorithm is terminated; otherwise, continue with Step 3.

3) Compute the singular-value decomposition of $\underline{J}^{(k)}$:

$$\underline{J}^{(k)} = \underline{U} \begin{bmatrix} \underline{S} \\ \underline{0} \end{bmatrix} \underline{V}^T .$$

4) Partition the diagonal matrix $\underline{s}$ such that $\underline{s}_1$ = diag $(s_1, s_2, \ldots, s_r)$ and $\underline{s}_2$ = diag $(s_{r+1}, s_{r+2}, \ldots, s_n)$, where r is the grade of the matrix $\underline{J}$. If s_ℓ is the last nonzero singular value of $\underline{J}$, then the grade r selected is that for which

$$s_1/s_r + s_{r+1}/s_\ell < s_1/s_j + s_{j+1}/s_\ell,\ j=1,\ 2,\ \ldots,\ \ell-1.$$

Partition $\underline{V} = [\underline{V}_1,\ \underline{V}_2]$ similar to $\underline{s}_1,\ \underline{s}_2$.

5) Compute the Gauss-Newton direction in the space spanned by $\underline{V}_1$:

$$\underline{p}_1 = -\ \underline{V}_1\ \underline{s}_1^{-1}\ \tilde{\underline{f}}_1$$

where

$$\underline{f}^T\underline{U} = [\tilde{\underline{f}}_1^T\ \tilde{\underline{f}}_2^T\ \tilde{\underline{f}}]\ .$$

6) If the relative decrease in the function $F(\underline{x})$ is greater than 1%, a correction to the Gauss-Newton direction is not required, set $\underline{p}_2 = 0$ and continue at Step 7. Otherwise, compute the matrices $\underline{Y} = \underline{V}_2^T\ \underline{B}^{(k)}$ (where $\underline{B}\ (\underline{x}) = \sum_{i=1}^{n} f_i(\underline{x})\ \underline{G}_i(\underline{x})$ and $\underline{G}_i(\underline{x})$ is the Hessian matrix of $f_i(\underline{x})$) and $\underline{Q} = \underline{Y}\ \underline{V}_2$. Use the modified LDL^T factorization (modified Cholesky factorization [25]) to solve the equations $(\underline{s}_2^2 + \underline{Q})\ \underline{y} = -\underline{s}_2\ \tilde{\underline{f}}_2 - \underline{Y}\ \underline{p}_1$ and set $\underline{p}_2 = \underline{V}_2\ \underline{y}$.

7) Set $\underline{p}^{(k)} = \underline{p}_1 + \underline{p}_2$. Let $\sigma > 0$ be a small preassigned scalar. If $-\underline{g}^{(k)T}\underline{p}^{(k)}/(||\underline{g}^{(k)}||\ ||\underline{p}^{(k)}||) < \sigma$ and $r > 0$, then set $r = 0$ and return to Step 5 to recompute $\underline{p}^{(k)}$.

8) Perform a one-dimensional minimization (such as cubic interpolation [26]) to find the optimal step length $\alpha^{(k)}$, i.e., $F(\underline{x}^{(k)} + \alpha^{(k)}\underline{p}^{(k)}) \cong \min_{\alpha} F(\underline{x}^{(k)} + \alpha\underline{p}^{(k)})$.

9) Compute $\underline{x}^{(k+1)} = \underline{x}^{(k)} + \alpha^{(k)}\underline{p}^{(k)}$, $\underline{f}^{(k+1)}$, $\underline{J}^{(k+1)}$ and $\underline{g}^{(k+1)}$; set $k = k+1$ and continue at Step 2.

Further details of the CGN algorithm and its analytical derivation are given by Gill and Murray [28]. The technique is found to be safeguarded, robust and reliable in this investigation. The details of the computer program 'CGN' are provided in Appendix A. The results obtained using the CGN method will be discussed in Chapter VII.

CHAPTER V. STRESSED SYSTEMS

Stability Study in the Stressed Systems

In the application of the transient energy function (TEF) method commonly made [7, 8], the power system is usually moderately loaded (i.e., unstressed); the system is brought to instability by an increased disturbance magnitude (e.g., longer fault duration). The limiting conditions of interest (e.g., critical interface power flow and plant generation) are usually dependent on the location and the duration of the disturbance, and by the power generation of plants close to the disturbance. The transient behavior of such medium size networks is often easy to predict by the TEF method. If the magnitude of the disturbance is large enough, the generators close to the location of the disturbance will separate from the system.

In power system operation and planning, stressed conditions arise due to increased power transfers and heavy loading of transmission systems [4]. In such a situation, when a large disturbance of short duration occurs, the disturbance may be cleared by losing a key transmission facility. In some extreme situations of transmission inadequacies, the post-disturbance system may not even be steady-state stable. When the post-disturbance system is steady-state stable, it is of interest to a power systems analyst to study the transient behavior of the system.

A typical stability study of interest in the operation of the stressed systems is arriving at the transient stability limits in terms

of critical transmission interface power flow limits and critical plant generation limits [2]. Such a study is aimed at computing the guidelines for operating limits of certain power flow or generation, constrained by the stability of the system.

For a stressed system, the post-disturbance is often characterized by the weak synchronizing forces [6, Chapter 3] caused by large transmission impedances. In these cases, the transient behavior of the system is complex to predict. The critical power flow or generation may be limited by the system's splitting up at a point in the network away from the plants closer to the disturbance location. In this case, if and when the instability occurs, it will take place as a separation of a large group of generators from the rest of the system (which includes the most severely disturbed generators that are close to the disturbance location). This is the so-called inter-area mode phenomenon of the stressed systems, which was observed in the Ontario Hydro System in Canada.

In this research investigation, the inter-area mode of instability was carefully observed in the time-simulation to develop an understanding of its dynamics and its implications in the TEF method. The inter-area mode phenomenon can be described as follows. Following a large disturbance, a small group of generators close to the fault location are severely disturbed initially. During the initial part of the transient, the inertial response of this small group dominates as an evidence of the immediate effect of the disturbance. The early part of the transient can only be characterized by the situation of

this small group tending to separate from the rest of the system. But, as the transient progresses, the weak synchronizing forces in the system dominate. If instability occurs, it takes place as a separation of a large group of generators, which includes the small group severely disturbed initially. The large group's separation from the rest of the system is observed to be a slow process and the system splits up after 2-3 seconds elapse from the instant of removal of the disturbance ($t_{c\ell}$). The large transmission impedances and the heavy loading of certain critical plants create weak synchronizing forces at a transmission interface, separating a large group of generators from the rest of the system. Thus, this weak synchronizing forces cause many more generators than the generators disturbed initially to separate from the rest of the system.

When the transient stability analysis is made by conventional means, the time simulation must be run for a long enough period (3 seconds) to detect the nature of system separation. Analysis of such instability phenomena by the TEF method is a complex task. A host of analytical and numerical issues are encountered and must be dealt with.

Implications of Inter-area Mode in the TEF Method

Extending the TEF method to the study of complex instability phenomena of inter-area mode involves dealing with the following main issues:

1) Determination of the mode of disturbance (MOD) and
2) Unstable equilibrium point (UEP) solution.

The description of the key problem is as follows. The UEP solution technique starts with the ray point of a few machines advanced, corresponding to the initial MOD selected. The robust technique, like the CGN method, converges to the UEP with many more generators advanced. The final MOD, as noticed in the UEP, checks with the nature of system separation observed in the conventional time simulation.

The scheme for determining the MOD (Chapter III) accurately predicts the mode of disturbance in the UEP of interest in the case of unstressed systems. The mode of disturbance selected by this scheme in the stressed cases usually consists of machines which are electrically close to the disturbance location and severely disturbed initially. Obtaining the UEP solution is a nontrivial task, due to the severe numerical ill-conditioning caused by the stress. The UEP solution obtained using the MOD selected, however, contains many more advanced generators, indicating the existence of the inter-area mode of system separation. To confirm the validity of the UEP solution obtained, the following key issues require verification and a thorough examination:

1) The apparent shift in the mode of disturbance has to be justified and explained. The UEP solution, with a large group of generators advanced, must be verified to be a proper UEP for stability assessment.

2) In some extreme cases of stress, no UEP solution is obtained. In such situations, the post-disturbance system must be verified to be steady-state unstable.

3) The UEP solution algorithms, such as the Scaled Newton-Raphson (SNR), and DFP methods experience a slow convergence or divergence in obtaining the UEP for inter-area mode cases. The numerical ill-conditioning caused by the stress in the system has to be dealt with, to accurately obtain the UEP of interest.

UEP Justification

The test for verifying the UEP in the case of inter-area mode was developed based on the following physical reasoning. A careful analysis of data showed that for a given system, for the same disturbance, the characteristic differentiating the unstressed system from the stressed system was the loading at certain generators. In the unstressed case, the MOD selected initially was confirmed in the UEP solution obtained finally. In the stressed case, the UEP obtained was that of the inter-area mode type and the shift in the MOD needed to be verified.

The predisturbance and the post-disturbance network configurations were identical in both the cases. The weak synchronizing forces in the stressed case were caused by the increase in power generation in a certain power station. This resulted in machines other than those predicted by the initial determination of MOD to separate from the system in the post-disturbance period. Incorporating this important physical feature (a certain plant being heavily loaded in the stressed case) in the UEP verification test was attempted.

In the case of inter-area mode, the separation of a large group of generators and the shift in MOD were observed to be a very slow process (after 2 seconds or so) in the post-disturbance period. Hence, it was attempted to investigate the post-disturbance stable equilibrium for a perturbation in the generation of a certain critical plant. The aim is to identify the coherent machines in the post-disturbance system by introducing a small change in its critical electrical quantity that primarily caused the stressed conditions in the system.

The UEP verification procedure is as follows. It is assumed the analyst will have implicit knowledge of the machines which are heavily loaded in the system. Having obtained the UEP, the aim of the test is to verify whether the UEP is the correct one for the given disturbance and the post-disturbance system. If the predicted mode of disturbance is the same as the MOD in the UEP, this test will not be done. Let

n = total number of machines,

m_i = number of machines included in the MOD $\{m_1, m_2, \ldots, m_i\}$,

ℓ = number of machines that are heavily loaded $\{\ell_1, \ldots, \ell_\ell\}$,

m_f = number of machines advanced in the actual UEP solution,

$\underline{\theta}^{s1}$ = predisturbance stable equilibrium point, and

$\underline{\theta}^{s2}$ = post-disturbance stable equilibrium point (SEP).

1) Determine the machines which are advanced at $\underline{\theta}^{s2}$ ($\underline{\theta}^{s2}$ list).

   a) Find $\theta_k = \min \{\theta_i^{s2}\}$ $i=1, 2, \ldots, n$.

   b) List all machines j, for which $\theta_{jk}^{s2} > \frac{\pi}{2}$ and $\theta_j^{s2} > \theta_j^{s1}$.

   This list provides an indication of all machines which are advanced at the post-disturbance SEP.

2) Determine the effect of the loaded machines on the post-disturbance SEP.

   a) Apply a perturbation $\Delta P_{m_{\ell_i}}$ = 1 PU or 10% of actual generation (whichever is smaller) to machines $\ell_1, \ell_2, \ldots, \ell_\ell$.

   b) Find $\Delta\underline{\theta}^{s2} = -[\underline{J}]^{-1}_{|\underline{\theta}^{s2}} \cdot \underline{f}(\underline{\theta}^{s2}, \Delta\underline{P}_m)$ where $\underline{J}$ is the Jacobian of $\underline{f}$ and $\underline{f} = [f_1, f_2, \ldots, f_n]^T$, where f_i is given in Eq. (4.5).

   This list ($\Delta\underline{\theta}^{s2}$ list), gives information on how the post-disturbance system is affected by the heavily loaded machines. It also incorporates the effect of the network parameters via the terms of the Jacobian matrix.

3) From the UEP solution obtained, prepare a list of the advanced machines.

4) Compare the list generated in step 1 ($\underline{\theta}^{s2}$ list) with the list of advanced machines at the UEP, and sort the machines in the following manner:

   $\{j_1, j_2, \ldots, j_j\}$ machines in $\underline{\theta}^{s2}$ list, but not in the UEP list.

   $\{k_1, k_2, \ldots, k_k\}$ machines in the UEP list, but not in the $\underline{\theta}^{s2}$ list.

   This sorting detects machines which have large θ_i^{s2} angles, but do not advance in the UEP.

5) The last step in the test is to justify the presence of $\{k_1, k_2, \ldots, k_k\}$ in the UEP list. Remove machines $\{j_1, \ldots, j_j\}$ from the $\Delta\underline{\theta}^{s2}$ list and sort the $\Delta\underline{\theta}^{s2}$ list. Check whether the first m_f machines of the $\Delta\underline{\theta}^{s2}$ sorted list are identical to the machines in the UEP list. If the lists tally, the UEP is a valid UEP and correctly describes the post-disturbance configuration of the stressed system.

It may be worthwhile to note that the calculation of $\Delta\underline{\theta}$ in step 2(b) is the same as the provision provided in SNR and CGN methods for computing the direction of search for UEP or SEP calculation.

In some cases of the stressed systems, the UEP solution could not be obtained. In such situations, the post-disturbance system was found to be steady-state unstable. In other words, the so-called post-disturbance stable equilibrium obtained may itself be steady-state unstable to start with. In such situations, where the UEP could not be computed, it is necessary to check the post-disturbance system for a possible steady-state instability. In this investigation, the following methods were attempted to identify steady-state instability of the post-disturbance system:

1) Lyapunov's indirect method [29, Chapter 5] and

2) Computation of synchronizing power coefficients [6, Chapter 3].

Lyapunov's indirect method requires the post-disturbance system be linearized over the equilibrium point under scrutiny. The resulting linear system is given as

$$\dot{\underline{X}} = \underline{A}\,\underline{X} \tag{5.1}$$

where

$$\underline{X} = \begin{bmatrix} \tilde{\omega} \\ \cdots \\ \theta \end{bmatrix}, \quad \underline{A} = \begin{bmatrix} \underline{0} & \vdots & \underline{M}^{-1}\underline{J} \\ \cdots & \vdots & \cdots \\ \underline{I} & \vdots & \underline{0} \end{bmatrix}$$

$$\underline{M} = \text{Diag}\,[M_1, \ldots, M_n],$$

$$\underline{J} = [\frac{\partial f_i}{\partial \theta_j}],\ i, j = 1, \ldots, n\ ,$$

and $\underline{f}(\underline{\theta})$ is the vector of accelerating powers as in Eq. (4.5) and M_i, θ_i and ω_i are inertia, angle and angular velocity, respectively, for a generator i. Any positive real eigenvalue of $[\underline{M}^{-1}\underline{J}]$ will indicate that the post-disturbance system is steady-state unstable. Subsequently, there is no need to find the UEP for transient stability assessment. The $[\underline{J}]$ matrix required for this analysis is the same as the one being computed in the SNR and CGN methods for the SEP or UEP solutions.

The synchronizing power coefficient is defined as

$$P_{s_{i,j}} = \frac{\partial P_{ei}}{\partial \theta_{ij}}\bigg|_{\underline{\theta}^s} \tag{5.2}$$

where P_{ei} is the electric power of generator i as given in Eq. (2.2), $\theta_{ij} = \theta_i - \theta_j$, and $\underline{\theta}^s$ is the post-disturbance SEP. It is simplified as

$$P_{s_{i,j}} = (C_{ij}\cos\theta_{ij} - D_{ij}\sin\theta_{ij}) \tag{5.3}$$

where C_{ij} and D_{ij} are as defined in Eq. (2.2), and it is interpreted

as the change in the electrical power of the ith machine due to the change in the angle between machines i and j. The negative values of $P_{s_{i,j}}$ imply the post-disturbance system is steady-state unstable.

The results of UEP verification and justification of absence of UEP are provided in Chapter VII.

Numerical Ill-conditioning of the Stressed Systems

In this research investigation, it was observed that the stressed systems were associated with severe numerical ill-conditioning, with regard to computing the UEP solutions. Especially in the cases involving the inter-area mode of transient behavior, the numerical techniques were found to be vulnerable to divergence or very slow convergence to the UEP solution of interest. A wrong UEP will lead to a subsequent incorrect stability assessment. It is essential that the UEP solution technique must be robust and safeguarded against divergence, in order to rely on the UEP solution obtained.

The numerical problems caused by the numerical ill-conditioning have been dealt with in Chapter IV. For the same system studied, the unstressed situations did not cause any severe numerical ill-condition. Only in the stressed situations, the severe numerical ill-conditioning and the divergence of the solution techniques were observed. For highly stressed systems, the potential energy surface can be very steep in certain directions and very shallow in other directions. The stressed systems are large realistic power networks operated close to their stability limits. Attempts were made in this

investigation to understand the effect of stress on the potential energy surfaces. Figures 5.1 and 5.2 are provided to illustrate the influence of a critical plant generation over the potential energy surfaces in the stressed systems. These figures will be referred to as cases A and B, respectively. The loading of the machine i in case B is 250 MW higher than that of case A. Both the cases of a 50-machine stressed system are subjected to the same disturbance and have the same post-disturbance network with the only difference being the generation of the machine i. The CGN method (Chapter IV) is used to determine the desired UEP in both the cases. The numerals on the figures indicate the position at each iteration of the CGN method, along with the starting point and the final UEP converged to. A graphics package (AGRAPH) and a procedure for multidimensional interpolation to exactly fit the significant points are made use of. The potential energy plots on the vertical axis, with respect to a pair of machine angles, are obtained (refer to [30] for more details on obtaining the plots).

In Figure 5.2 of the more stressed, case B, the potential energy surface in the vicinity of the UEP is more irregular, compared to case A, influenced by the higher stress on the system. The higher stress in the system is indicated in Figure 5.2 by a steeper potential energy surface near the UEP.

In such stressed situations, the following numerical issues were encountered:

1) Mismatch functions ($\underline{f}(\underline{\theta})$ of Eq. (4.5)) exhibit widely different sensitivities with respect to various variables (machine

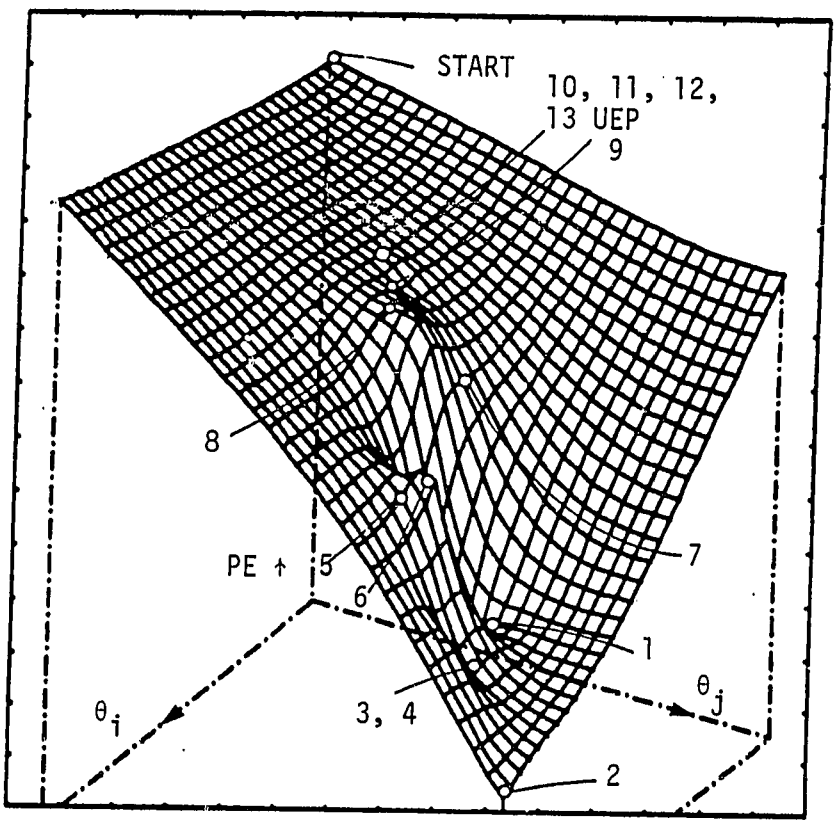

Figure 5.1. Case A: Potential energy plot for machines i, j

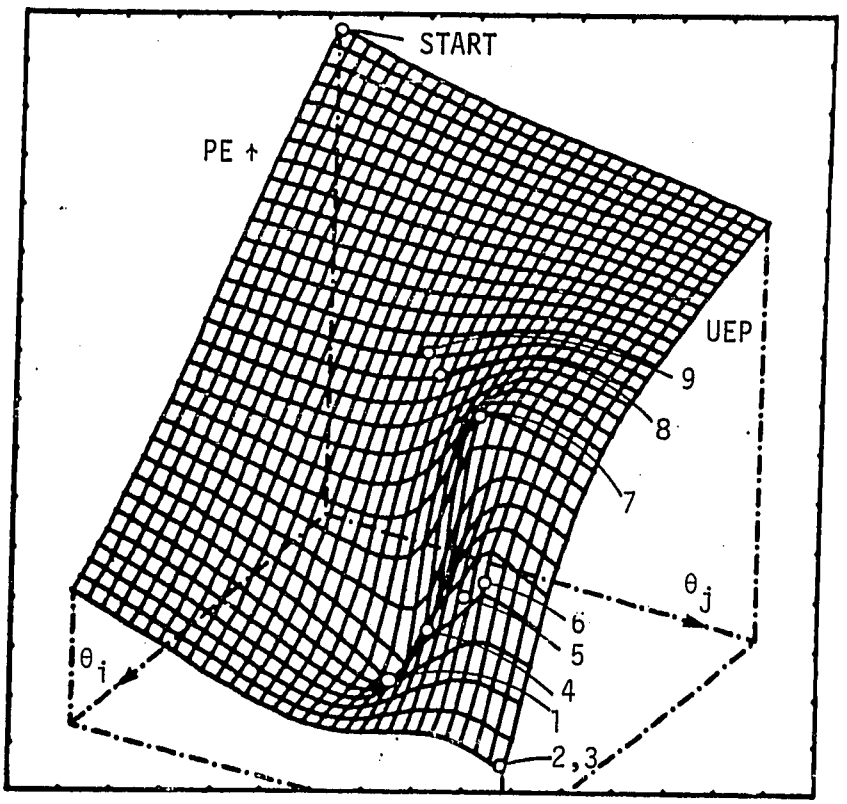

Figure 5.2. Case B: Potential energy plot for machines i, j

angles). This will contribute to an irregularity in the functional surfaces being iterated upon. This feature is originally caused by the irregularities of potential energy surface near the UEP, which is otherwise smooth in the unstressed cases. The scaling of variables performed in the SNR method can improve, substantially, the rate of convergence to the UEP solution desired.

2) In some extreme cases of ill-conditioning, especially in the cases of inter-area mode, the SNR method was observed to be divergent; the DFP method was extremely slow and diverged in some cases; the CGN method invariably took several correction steps that requires the computation of second derivatives of accelerating powers. The correction steps imply severe numerical ill-conditioning [28] and are taken only when the solution cannot progress with only the first derivative information.

The CGN method (Chapter IV), developed in this investigation, was found to be robust and reliable in the cases involving the inter-area mode.

CHAPTER VI. TEST SYSTEMS

The developments made in this investigation were examined by testing them on the following systems:

Modified Iowa System (MIS) with an unstressed network.

Ontario Hydro (OH) system with the network in stressed and unstressed operating conditions.

MIS System

Figure 6.1 shows the main high voltage lines of the 17-generator MIS system. It is a reduced Iowa network. This test system was mainly selected for the complexity of the mode of the disturbance (MOD). A cluster of unstable equilibrium points of similar energy levels is present near the post-disturbance trajectory, when a three-phase fault near the Fort Calhoun generator (Bus #773) is cleared by opening line (773-339).

Ontario Hydro System

This is the main test system used in this study. The operating conditions when the network is stressed are of prime interest in this investigation. The position of this power system, showing the critical generators of the NANTICOKE and BRUCE complex, is provided in Figure 6.2. In this investigation, the 'unstressed situation' can be typically referred to a condition when the BRUCE (nuclear) units are not heavily loaded. The 'stressed situation' represents the condition of heavy

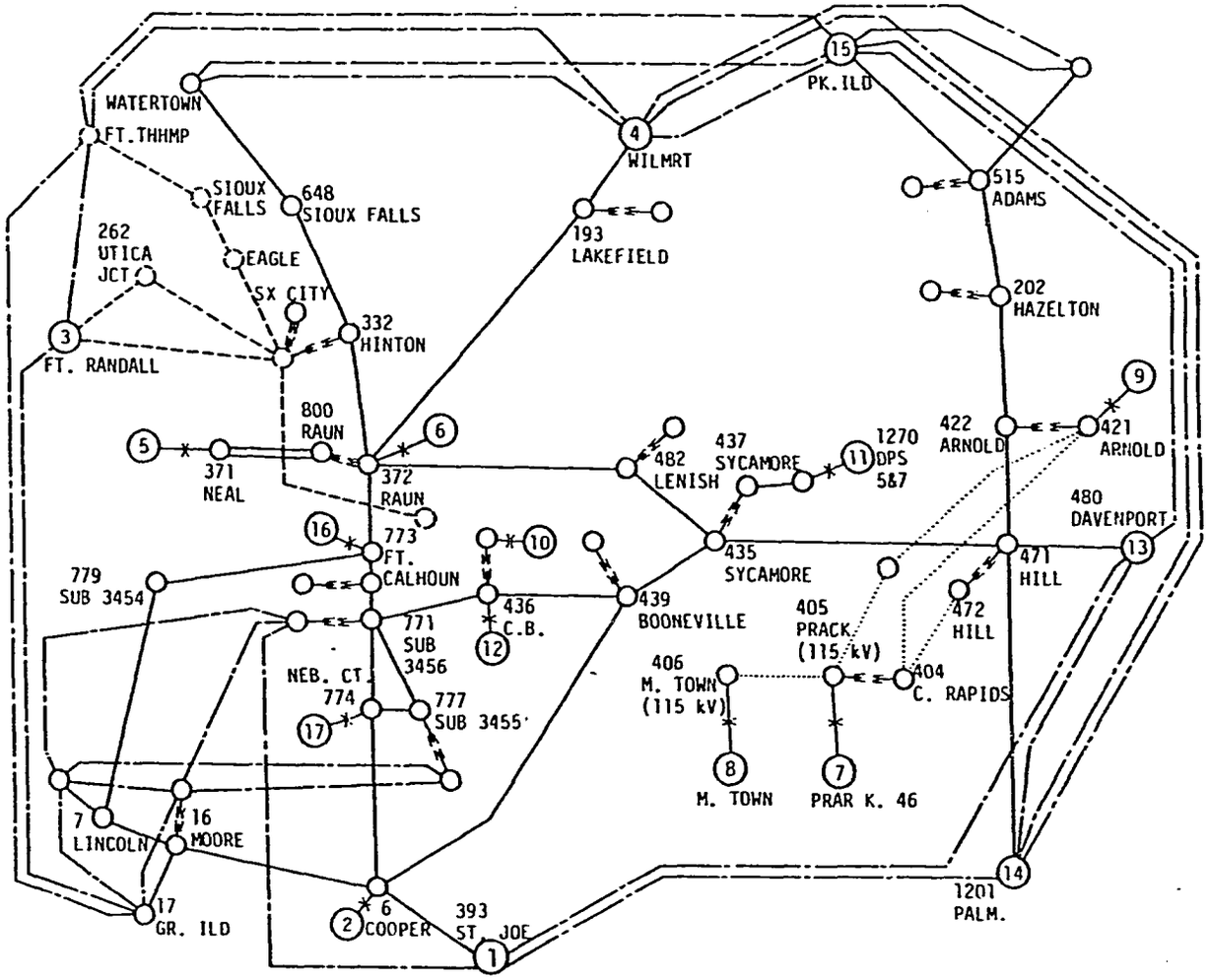

Figure 6.1. 17-generator Modified Iowa System

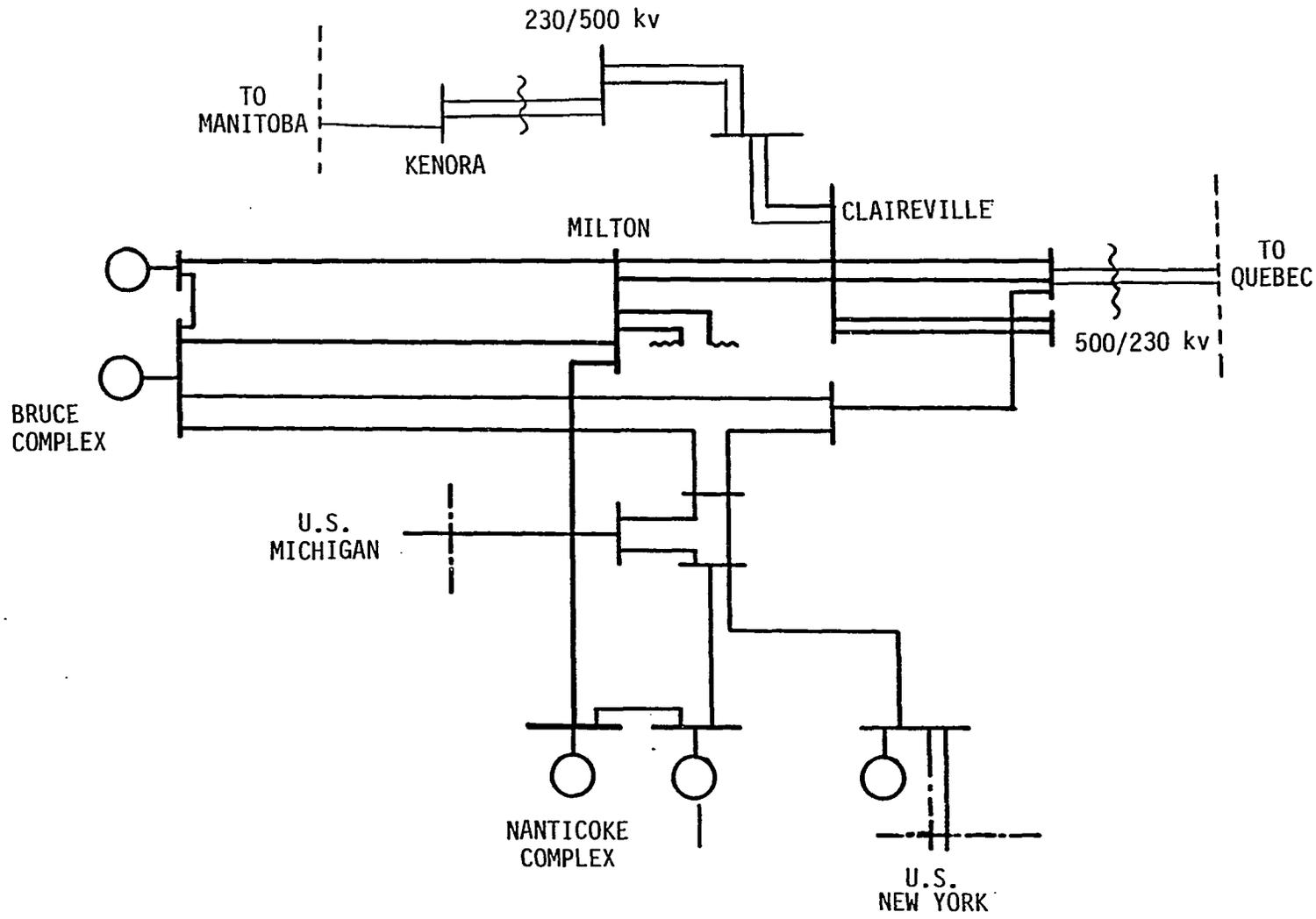

Figure 6.2. Portion of Ontario Hydro System showing the critical generators

generation schedule at the BRUCE units, causing the transmission lines in this part of the network to be heavily loaded. The large disturbance is introduced close to the NANTICOKE or BRUCE complex. It is a fault at NANTICOKE or MILTON bus, cleared by opening a 500 kv transmission line.

The stability limits of interest are the generation at the BRUCE and NANTICOKE complex, which are constrained by transient stability considerations. In many cases, the initial and post-disturbance conditions selected for the study represent highly stressed power system conditions. During this investigation, the emphasis was mainly given to the analysis of scenarios that arise when the transient stability limits of critical plant generations or power flows at certain transmission interfaces are being computed.

The following sizes of the reduced OH systems were studied for different scenarios in stability assessment:

- a 17-generator system,
- a 50-generator system,
- a 100-generator system, and
- a 115-generator system.

The results obtained will be discussed in Chapter VII.

CHAPTER VII. SIMULATION STUDIES AND RESULTS

Introduction

The transient stability assessment using the transient energy function (TEF) method specifically requires determination of the following:

1) Parameters of the post-disturbance system and the post-disturbance stable equilibrium ($\underline{\theta}^s$) generator angles.
2) Angles and speeds ($\underline{\theta}^{c\ell}$, $\underline{\tilde{\omega}}^{c\ell}$) of the generators at the end of the disturbance period, $t_{c\ell}$.
3) Identification of the controlling unstable equilibrium point ($\underline{\theta}^u$) for the disturbance under investigation.
4) Critical energy, V_{cr}, for the disturbance under investigation, which is V^u; the energy margin, $\Delta V = V^u - V^{c\ell}$, is then computed as an index of robustness.

The various computations involved in transient stability assessment using the TEF method are summarized in Figure 7.1.

In applying the above-mentioned procedure to stressed large-scale systems, the following analytical and numerical enhancements of the basic procedure were implemented and tested:

1) Automatic determination of the mode of disturbance (MOD) for characterizing the controlling UEP. Determination of MOD is required for identifying which particular group of generators will be more advanced than the others (generally, angles > $\pi/2$, for the situation where the disturbance causes these generators

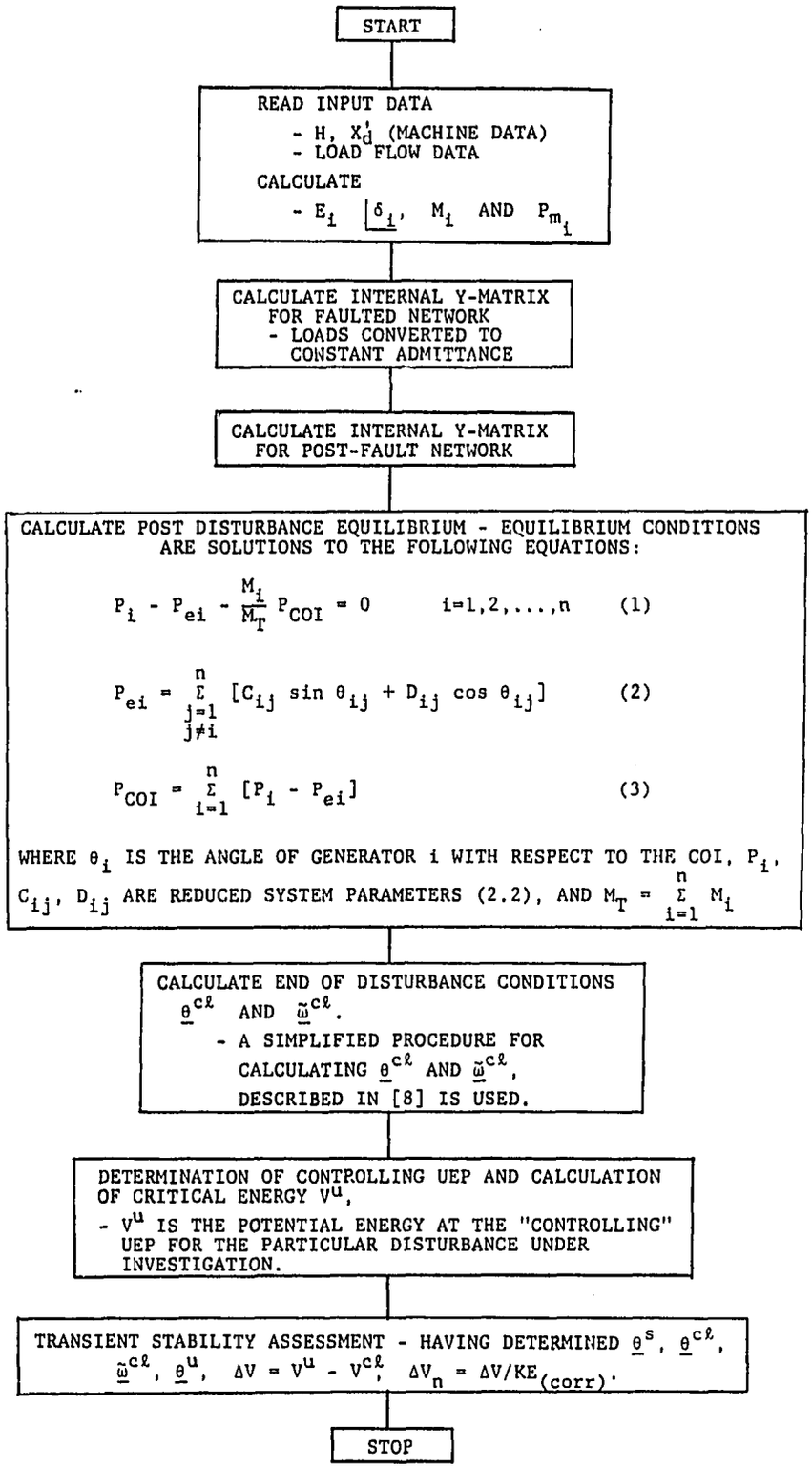

Figure 7.1. Flow chart of transient stability assessment

to accelerate) in the UEP of interest. Specifically, a scheme to select the candidate modes of disturbance to identify the MOD correctly (discussed in Chapter III).

2) A reliable and robust algorithm based on the Corrected-Gauss-Newton method (CGN) for the computation of the controlling UEP. Reliable starting points (ray point) for the UEP solution, for a given MOD (provided in Chapter IV).
3) Verification of the UEP solution obtained in the case of inter-area mode of transient behavior. In this case, there will be a shift in the MOD and a large group of generators split from the system (including the most severely disturbed generators, initially). Justification if no UEP solution is obtained in the extremely stressed situations that lead to steady-state instability. These efforts are explained in Chapter V.

These three modifications of the basic TEF procedure were aimed at improving the TEF method to suit the realistic situations that arise in the analysis of stressed large-scale power system operation, i.e., heavy loading of the critical power plants combined with the limitations in transmission.

The new developments (automated MOD determination, CGN method and UEP verification scheme) were tested for different scenarios in several stressed, large and realistic power networks. The reliability and the efficiency of the procedure were the two aspects that were closely examined. The details of the test networks and the areas of study are

provided in Chapter VI. The test systems were the following:

1) Modified Iowa System - 17-generator system.

2) Ontario Hydro System - 17-, 50-, 100- and 115-generator systems.

This chapter summarizes and discusses the key results obtained in the validation phase of this research endeavor.

MOD Determination - Results

A scheme for automating the MOD determination is provided in Chapter III. The details of the computer program MOD developed in this investigation are provided in Appendix A.

The MOD determination scheme was tested for the following types of disturbances:

1) A case of complex mode of disturbance in a medium size unstressed system.
2) Simple modes of disturbance in large unstressed networks.
3) Simple or complex initial modes of disturbance, followed by the inter-area mode of separation in stressed large-scale systems.

The networks of study vary from medium to large size (17-generators to 115-generators system).

Tables 7.1 - 7.7 display the key results of the MOD determination scheme. The candidate modes of disturbance listed (column 2 of these tables) are different groupings of generators ranked according to effect of disturbance (i.e., sorted $KE_{(corr)}$ list in step A-3 of the procedure provided in Chapter III). The $KE_{(corr)}$ values represent the

portion of the transient kinetic energy that tends to split the corresponding group of generators (mode) from the rest of the system. The MOD test is performed to identify the controlling UEP among the selected candidate modes. The selected MOD is the candidate with the least value of $\Delta V_{PE}|_n = \Delta V_{PE}/KE_{(corr)}$. The MOD predicted by the scheme in each of these cases corresponds to the underscored $\Delta V_{PE}|_n$ in the last column of Tables 7.1 - 7.7. The summary of individual results in the cases of study are the following.

Unstressed systems

1) In Fort Calhoun case of the 17-generator Modified Iowa System (Table 7.1), the MOD predicted consists of seven generators. This is a benchmark case of study investigated earlier [9]. In this case of study, the identification of the controlling UEP is complicated by the presence of a cluster of UEPs of similar energy levels that are present near the post-disturbance trajectory. This is a case where the appropriate critical energy level is determined by these seven generators, among which only a few lose synchronism initially for a critically cleared disturbance. The final UEP solution obtained has the same MOD that was predicted. The UEP solution obtained provided a stability assessment that agreed with the conventional time simulation.
2) The Ontario Hydro (OH) 50-generator system with the NANTICOKE generation at 3600 MW (Table 7.2) and the OH

Table 7.1. MOD determination in the MIS 17-generator system, Fort Calhoun case - unstressed system

System and case of study	Selected candidate modes of disturbance	No. of machines in the mode	$KE_{(corr)}$	ΔV_{PE}	$\Delta V_{PE}\|_n$
Modified Iowa 17-generator system	1	7	1.9531	29.6730	15.1926[a]
Fort Calhoun case	2	6	1.8311	32.1244	17.5441
3ϕ fault at Fort Calhoun (Bus No. 773) cleared by opening line 773-339 at 0.1 seconds	3	5	1.5173	31.7371	20.9171
	4	3	1.0368	25.8197	24.9042
	5	2	0.5397	19.7020	36.5033

[a]MOD selected: candidate 1, comprised of machines 12, 10, 16, 6, 5, 17 and 2. (2 Council Bluffs, Fort Calhoun, 2 Neal, Nebraska City and Cooper machines.)

Table 7.2. MOD determination in the OH 50-generator system, NANTICOKE 3600 MW - unstressed system

System and case of study	Selected candidate modes of disturbance	No. of machines in the mode	$KE_{(corr)}$	ΔV_{PE}	$\Delta V_{PE}\|_n$
Ontario Hydro 50-generator system NANTICOKE 3600 MW case 3ϕ fault on NANTICOKE 500 kv bus, cleared by opening line NANTICOKE-MILTON at 0.108 seconds	1	2	2.4688	10.12029	4.0993[a]
	2	7	1.7277	38.9171	22.5256
	3	4	1.7200	25.8736	15.0431
	4	5	1.7179	31.6053	18.3977
	5	10	1.1581	51.8434	44.7655

[a]MOD selected: candidate 1, comprised of machines 20 and 26. (2 NANTICOKE machines.)

100-generator system with the BRUCE generation at 1500 MW (Table 7.3) are large systems with simple modes of disturbance. The MOD in the final UEP solution is the same as the MOD predicted. The stability assessment using this UEP was confirmed by the conventional time simulation.

In Tables 7.1 - 7.3, the MOD predicted was the first candidate on the sorted $KE_{(corr)}$ list and hence, would have been reliable for any cut-off value chosen for the length of the list.

3) A notable feature was observed in the OH 50-generator system with BRUCE generation at 1800 MW (Table 7.4). The MOD predicted is the 26th candidate in order of the corrected kinetic energy ranking. For the scheme to be reliable in this case, the cut-off value of $KE_{(corr)}$ (step A-3 of the procedure in Chapter III) should be less than 50% of the maximum value of $KE_{(corr)}$ in the list. These three machines characterize the UEP closest to the post-disturbance trajectory. The final UEP solution corresponds to the predicted MOD. This UEP gave a stability assessment that agrees with the time simulation.

This case demonstrates the efficacy of the proposed procedure. In order to ensure the reliability of the procedure, careful selection of the cut-off value of $KE_{(corr)}$ should be made. It is recommended that the scheme must always include one or two additional candidate groups among the top one or two power stations appearing in the list of key machines (obtained in step A-1-d) of the procedure in Chapter III).

Table 7.3. MOD determination in the OH 100-generator system, BRUCE 1500 MW case - unstressed system

System and case of study	Selected candidate modes of disturbance	No. of machines in the mode	$KE_{(corr)}$	ΔV_{PE}	$\Delta V_{PE\|n}$
Ontario Hydro 100-generator system BRUCE 1500 MW case 3ϕ fault at bus BRUCE 2A (230 kv) cleared by opening line BRUCE 2A-HANON J2B at 0.108 seconds	1	3	1.7650	3.2798	1.8582[a]
	2	2	1.5232	5.9607	3.9134
	3	5	1.2237	31.0958	25.4104
	4	8	0.9030	46.7471	51.7695
	5	7	0.9026	40.7002	49.0925

[a]MOD selected: candidate 1, comprised of machines 58, 20 and 33. (2 BRUCE and DOUGLAS machines, respectively.)

Table 7.4. MOD determination in the OH 50-generator system, BRUCE 1800 MW case - unstressed system

System and case of study	Selected candidate modes of disturbance	No. of machines in the mode	$KE_{(corr)}$	ΔV_{PE}	$\Delta V_{PE}\|_n$
Ontario Hydro 50-generator system BRUCE 1800 MW case 3ϕ fault on BRUCE 500 kv bus, cleared in 0.108 seconds (no line is cleared)	1	12	2.6515	35.1405	13.2530
	2	11	2.6356	35.7159	13.5511
	3	10	2.6140	30.0559	11.4982
	.	.	.	.	.
	.	.	.	.	.
	25	31	1.5442	254.1239	164.5663
	26	3	1.3717	2.5077	1.8282[a]

[a]MOD selected: candidate 26 comprised of machines 9, 25 and 15. (2 BRUCE and DOUGLAS machines, respectively.)

This is illustrated by the case described in Table 7.4, where the three machines in the predicted MOD happen to be the first three machines in the list of key machines.

Stressed systems

Tables 7.5 - 7.7 comprise the results of the MOD predicted for the cases involving the stressed large power networks. In these cases, the true mode of disturbance is a large group of generators splitting from the system due to the dominance of inter-area mode over the initial effect of the disturbance. The MOD predicted in these cases is invariably a small group of generators that are severely affected initially. The shift between the initial and the final modes of disturbance is closely examined in a later section of this chapter. The specific results of MOD prediction in stressed systems are the following:

1) In the OH 50-generator system with NANTICOKE generation at 3700 MW, the MOD selected (Table 7.5) comprises two NANTICOKE generators. The starting point (ray point) has these two machines advanced (angles > $\pi/2$). However, the CGN method of solution, when started with this point, converges to a UEP with 29 machines advanced (angles > $\pi/2$), which includes the two generators of predicted MOD. The time simulation confirmed this inter-area mode of separation of the 29 generators from the rest of the system.
2) In the OH 50-generator system with NANTICOKE generation at 3950 MW for the MILTON case (Table 7.6), the MOD predicted

Table 7.5. MOD determination in the OH 50-generator system, NANTICOKE 3700 MW case - stressed system with inter-area mode behavior

System and case of study	Selected candidate modes of disturbance	No. of machines in the mode	$KE_{(corr)}$	ΔV_{PE}	$\Delta V_{PE\|n}$
Ontario Hydro 50-generator system NANTICOKE 3700 MW case 3ϕ fault on NANTICOKE 500 kv bus, cleared by opening line NANTICOKE-MILTON at 0.108 seconds	1	2	6.4928	8.5407	1.3154[a]
	2	9	4.0974	16.8255	4.1063
	3	10	4.0854	17.3483	4.2464
	4	11	4.0842	21.1046	5.1674
	5	12	4.0752	16.5163	4.0529

[a]MOD selected: candidate 1, comprised of machines 20 and 26. (2 NANTICOKE machines.)

Table 7.6. MOD determination in the OH 50-generator system, NANTICOKE 3950 MW - BRUCE 3160 MW, MILTON case - stressed system with inter-area mode behavior

System and case of study	Selected candidate modes of disturbance	No. of machines in the mode	$KE_{(corr)}$	ΔV_{PE}	$\Delta V_{PE\|n}$
Ontario Hydro 50-generator system NANTICOKE 3950 MW case 3ϕ fault on MILTON 500 kv bus, cleared by opening line MILTON-CLAIRE at 0.108 seconds	1	12	10.8053	20.6643	1.9124
	2	11	10.7311	21.5488	2.0081
	3	10	10.6458	17.8673	1.6784
	6	15	10.6065	14.0218	1.3211
	7	16	10.6021	13.5105	1.2743[a]
	8	17	10.5897	13.6432	1.2884
	.	.	.	.	.
	.	.	.	.	.
	.	.	.	.	.
	17	24	9.0268	34.5419	3.8266

[a]MOD selected: candidate 7 comprised of machines 20, 26, 9, 25, 15, 21, 22, 17, 27, 14, 3, 16, 6, 19, 12 and 4. (2 NANTICOKE, 2 BRUCE, DOUGLAS, 2 PICKERING, 2 LAKEVIEW, DESJO, MCKAY, HOLDE, CANYO, LONOT, CHENA and HIGH FALLS machines, respectively.)

consists of 16 machines. The final UEP solution obtained with the CGN method has 29 generators advanced (angles > $\pi/2$) as opposed to the starting point with 16 machines advanced. The final MOD of 29 generators includes all 16 generators of the predicted MOD. The inter-area mode of system separation revealed by the conventional time simulation agrees with this UEP solution.

It may be worthwhile to note that the same 29 generators belonged to the inter-area mode of separation in the above-cited NANTICOKE cases. Interestingly, in both cases, the two BRUCE machines were heavily loaded with 3160 MW of generation; the transmission system has limitations caused by losing a 500 kv line. Thus, the initially predicted MOD is different in both the cases, but the final MOD in the UEP solutions of both the cases are the same. It illustrates the dominating effect of the inter-area mode present at that level of loading of the system.

To understand the shift in MOD, it must be recognized that the inter-area mode of system separation is a very slowly developing process (separation occurs after about 2 seconds). The weak synchronizing forces caused by the heavily loaded BRUCE machines and the large transmission impedances, finally dominate over the initial effect of the disturbance.

3) In the OH-115 generator system with BRUCE generation at 4800 MW case (Table 7.7), the predicted MOD comprises 19 generators. The CGN method, used to solve for the UEP, starting with the ray point of these 19 generators advanced

Table 7.7. MOD determination in the OH 115-generator system, BRUCE 4800 MW case - stressed system with inter-area mode behavior

System and case of study	Selected candidate modes of disturbance	No. of machines in the mode	$KE_{(corr)}$	ΔV_{PE}	$\Delta V_{PE\|n}$
Ontario Hydro 115-generator system BRUCE 4800 MW case 3ϕ fault on MILTON 500 kv bus, cleared by opening line MILTON-CLAIRE at 0.108 seconds	1	19	9.4573	29.0012	3.0665[a]
	2	22	9.2042	35.4695	3.8536
	3	21	9.1693	37.6871	4.1101
	.	.	.	.	.
	.	.	.	.	.
	.	.	.	.	.
	13	44	8.6769	38.0993	4.3909
	14	45	8.6401	38.3668	4.4405

[a]MOD selected: candidate 1 comprised of machines 21, 39-41, 47, 49, 29-31, 42-43, 26, 27, 38, 44, 32, 33, 46 and 48. (6 BRUCE, 5 NANTICOKE, 4 LAKEVIEW and 4 PICKERING machines, respectively.)

angles, converged to a UEP with 57 machines advanced. These 57 generators include all the 19 generators of the predicted MOD. This inter-area mode of system separation is confirmed by the time simulation.

Discussions

The CPU time required for the automatic determination of the MOD (for 10 candidates selected) in a 50-machine stressed system will be approximately equal to the same number of CPU seconds required for computing one actual UEP in the case of the inter-area mode. This provides a feel for the computational requirements of the MOD test.

The MOD prediction scheme was found to be reliable and reasonably efficient for the cases of study in this investigation. However, it is to be recognized that the scheme for selection of candidates is based on the following engineering judgement. The list of key machines provides a ranking of the machines according to the severity of the effect of disturbance on each machine at $t_{c\ell}$. At this stage, the severely disturbed groupings of the generators are to be selected as the candidate modes of the disturbance. If the i^{th} ranked machine (in the list of key machines) was to be in a candidate group of machines, it would have to include all the i-1 machines that are above it. Each of these i-1 machines are more severely disturbed than the i^{th} machine. If this engineering assumption is not made, it leads to an impractical way of considering all possible combinations of machines of candidate groups. Further efforts may need to be directed toward

finding the circumstances, if any, where this assumption may need improvement. The automated MOD selection scheme should be tested further in situations involving complex modes of disturbance.

CGN Method for UEP Solution - Results

In order to deal with the severe numerical ill-conditioning encountered in the heavily loaded stressed systems, the CGN method was attempted in the UEP solution. The basic algorithm of the Corrected-Gauss-Newton (CGN) method is provided in Chapter IV. The details of the computer program 'CGN' are furnished in Appendix A. The details of the nature of numerical issues encountered in this investigation are also discussed in Chapter IV.

The CGN method was tested for obtaining the UEP solutions for different operating conditions and different fault cases on five equivalents of the OH system. The performance of the method was closely examined along with the Scaled-Newton-Raphson (SNR) method and the Davidon-Fletcher-Powell (DFP) method. The SNR and DFP methods were developed elsewhere and are briefly outlined in Chapter IV. The CGN method uses first derivatives of the mismatch functions (Eq. 4.5) under normal situations. When the progress of the solution is not satisfactory, the second derivatives are explicitly computed. The numerical ill-conditioning is detected by monitoring the singular values of the Jacobian of the mismatch functions. The cause of the numerical ill-conditioning of the stressed systems are discussed in Chapter V. The SNR and DFP methods involve only the first derivatives of mismatch

functions. The DFP method approximates the second derivative information, without explicitly computing it, based on the progress made in the solution.

The three UEP solution techniques were specifically compared for speed in terms of CPU time, and reliability in terms of convergence to the correct UEP. In all the comparisons made, the three methods had identical starting points, and input/output data structure. Table 7.8 shows the result for three different systems. These systems are unstressed and had relatively simple mode of disturbance. The comparisons were performed on a VAX 11/8600 computer. Table 7.9 shows the results for three stressed cases. These comparisons were made on an AS/9 computer.

The results of Table 7.8 clearly show that for the unstressed case and simple mode of disturbance, the SNR method is superior to both CGN and DFP methods. The SNR method converges to the UEP quickly and reliably in these unstressed systems. However, in the stressed systems of Table 7.9, the CGN method is superior to both the SNR method and the DFP method. This is to be expected because the CGN method uses the second derivative information by explicitly computing it in some iterations of all these cases of Table 7.9. The CGN method produces the directions of search for the UEP based on grading the singular values to detect any ill-conditioning in any given iteration. An interesting feature about the SNR method is that it either converges or diverges very quickly.

Table 7.8. Comparison of UEP solution techniques for unstressed systems

Unstressed systems	SNR CPU sec.	Remarks	CGN CPU sec.	Remarks	DFP CPU sec.	Remarks
17-generator OH system	0.5	converged to correct UEP	1.5	converged to correct UEP	5.0	converged to correct UEP
50-generator OH system	11.5	converged to correct UEP	19.0	converged to correct UEP	23.0	converged to correct UEP
100-generator OH system	59.0	converged to correct UEP	370.0	converged to correct UEP	720.0	converged to correct UEP

Table 7.9. Comparison of UEP solution techniques in inter-area mode cases

Stressed systems	SNR CPU sec.	Remarks	CGN CPU sec.	Remarks	DFP CPU sec.	Remarks
50-generator OH system NANTICOKE 3950 MW case (inter-area mode)	2.1	failed to converge	11.0	converged to correct UEP	17.0	failed to converge
50-generator OH system NANTICOKE 3700 MW case (inter-area mode)	1.0	failed to converge	17.0	converged to correct UEP	18.0	failed to converge
115-generator OH system BRUCE 4800 MW case (inter-area mode)	3.4	failed to converge	31.7	converged to correct UEP	50.0	failed to converge

Discussions

1) Based on the results in this investigation, the ideal procedure to calculate the UEP would be to start with the SNR method; if solution progresses satisfactorily, continue with the method; if not, switch to the CGN method to obtain the solution.

2) As the system size increases, the DFP method is observed to be slower. In extremely ill-conditioned cases, it either converges very slowly or it fails to converge.

3) The CGN method was found to be very reliable in all the cases of numerical ill-conditioning encountered in this research effort.

4) The specific results of improvement to the starting points (ray point) can be summarized as follows. The ray point played an important role in the speed of convergence in the SNR method, if and when it converged. In the unstressed systems, the CGN method was insensitive to the starting points due to its robustness. However, in the stressed systems of inter-area mode behavior, the ray point played an important role in the reliability of convergence to the correct UEP.

5) To enhance the reliability further, it is recommended that the following provisions be included in the CGN method. If and when the updated quantity of $\Delta\underline{\theta}$ in each iteration has any $\Delta\theta_i$ more than 20°, a correction step of the CGN method can be forced and the direction of search can be based on the second derivative information. Extreme caution in such situations would slow down the method, but it may make the CGN method extremely reliable.

6) The CGN method requires a provision to store both the Jacobian and Hessian matrices in the computer memory. As the system size becomes very large (over 150 generators), the following problems can arise with ill-conditioned systems: a) massive storage requirements for the Jacobian and Hessian matrices, and b) computation of the Hessian can slow down the method significantly.

UEP Verification - Results

In the stressed large-scale systems, if instability occurs, the inter-area mode of system separation is observed. A small group of generators close to the disturbance tend to separate from the system initially. But, as the transient develops, a large group of generators separate from the system, including the initially disturbed small group. This phenomenon is due to the weak synchronizing forces present in the system, owing to the heavy loading of the system and the large transmission impedances. Chapter V discusses the analytical issues imposed by such complex transient phenomena. The inter-area mode is reflected in the UEP solutions obtained. This section provides the results of the UEP verification test developed in Chapter V. The UEP verification scheme was tested on two different test systems of the OH power network (50-generator and 115-generator systems). A sample result from each system is presented below.

OH 50-generator system

Portions of interest in this system are BRUCE and NANTICOKE power station complexes. In this system, the stressed condition is created by raising the BRUCE generation to 3160 MW. Generators 9 and 25 in the study are the two BRUCE machines. The stability limit of interest is the NANTICOKE generation. The generators 20 and 26 are the two NANTICOKE machines. The disturbance analyzed was a three-phase fault close to generators 20 and 26 of the NANTICOKE complex on the 500 kv bus.

Consider the situation where the NANTICOKE generation is at 3700 MW and the disturbance is cleared in 0.108 seconds by opening a 500 kv line. The automated MOD program selects the MOD to be generators 20 and 26 (refer to Table 7.6). Starting from the ray point corresponding to this MOD, the CGN method converged to a UEP in which 29 machines were advanced (generators 1-17, 19, 20-27, 33-35). Table 7.10 provides the comparison of the SEP and UEP to identify these 29 machines. The starting point (ray point) has machines 20 and 26 alone advanced. A careful analysis of the time simulation results was then conducted.

In Figures 7.2 and 7.3, the plots of machine angles of generators 20 and 26 with respect to the center of inertia (COI) of the system, their COI and the COI of 29 machine groups are displayed. Figure 7.2 is for the stable case ($t_{c\ell}$ = 0.108 seconds) and Figure 7.3 is for the critically unstable case ($t_{c\ell}$ = 0.1221 seconds). The time simulation results clearly showed that in the unstable case, 29 machines did separate from the system. The transient developed slowly and the separation occurred at about 2.5 seconds. Machines 20 and 26, the

Table 7.10. OH 50-generator system - NANTICOKE 3700 MW (inter-area mode) case, SEP and UEP solutions

Gen. No.	SEP (degrees)	UEP (degrees)	Gen. No.	SEP (degrees)	UEP (degrees)
1	49.1271	126.8573	26	74.5626	173.6037
2	32.504	113.0539	27	48.7384	140.2192
3	43.0345	128.1505	28	-0.5027	-3.0398
4	70.9245	153.2035	29	2.6166	6.2480
5	28.9799	113.3924	30	7.2711	16.7901
6	47.7590	137.5736	31	3.4536	9.6920
7	69.1294	139.6163	32	-39.2385	-27.2344
8	36.7080	123.2206	33	12.6067	86.0436
9	70.3327	164.9465	34	32.9026	105.4425
10	57.3249	135.4520	35	36.5604	115.7527
11	68.7278	143.8197	36	-17.0979	4.7819
12	37.7338	127.4462	37	-31.8327	-24.2887
13	42.5836	124.3910	38	-7.3191	-3.2712
14	53.2670	144.6421	39	13.7582	29.5758
15	65.2687	159.9028	40	-3.0988	-13.2800
16	48.8686	139.5303	41	39.4319	28.8230
17	39.9920	130.6347	42	12.9090	1.3141
18	33.8228	56.4415	43	-70.2783	-99.4906
19	47.9724	138.3286	44	4.2767	3.5292
20	75.6841	174.9556	45	-21.2720	-40.9582
21	55.5117	147.4498	46	1.1626	-5.0242
22	55.3599	147.1481	47	7.7970	11.7104
23	21.3893	100.8077	48	6.3929	5.7840
24	26.2527	110.7256	49	15.0216	1.9805
25	72.3695	167.6788	50	-7.8182	-23.0270

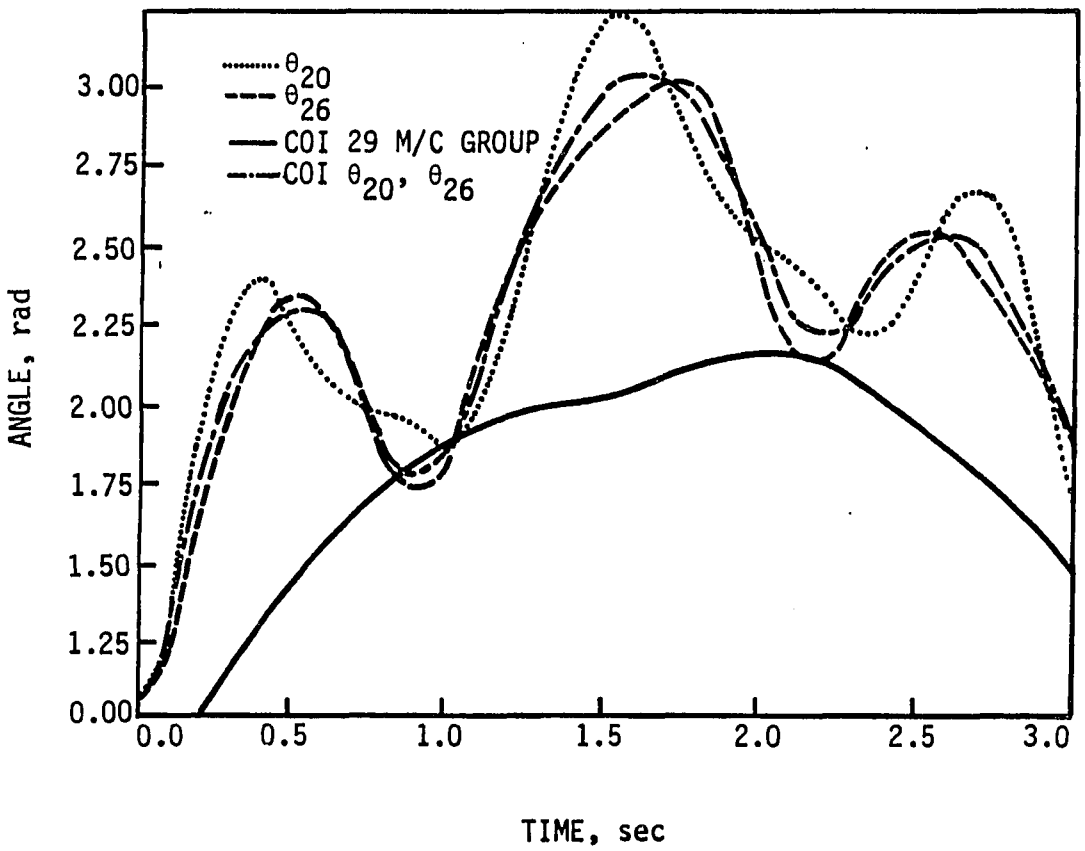

Figure 7.2. OH 50-generator system, NANTICOKE 3700 MW system - stable case

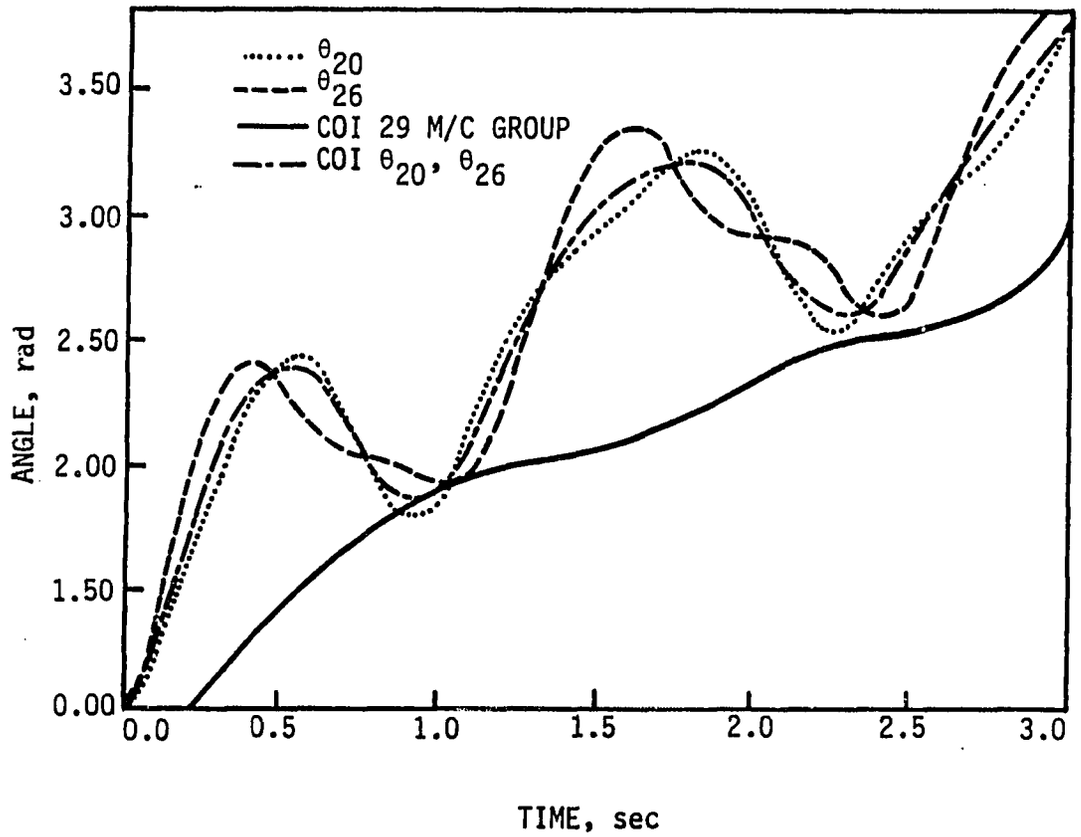

Figure 7.3. OH 50-generator system, NANTICOKE 3700 MW system - unstable case

initially disturbed machines, actually are stable in their first swing in Figure 7.3. If the simulation had not been conducted long enough, the results could have been misleading. On the other hand, the dominant mode, which is the inter-area mode described by the COI of 29 M/C group in Figure 7.3, clearly indicates the first swing instability for that mode. The UEP obtained correctly predicted this inter-area mode of separation. At the instant of removal of disturbance, the most severely disturbed generators are only 20 and 26. This is correctly determined by the automatic MOD selection procedure. As the transient progressed, the weak synchronizing forces in the post-disturbance period caused other machines to separate. Machines 20 and 26 could not lose synchronism without the other 27 machines separating. This physical phenomenon was accurately reflected by the UEP solution. In spite of starting from a point corresponding to the MOD for machines 20 and 26, the UEP converged to a solution with 29 machines advancing. The ray point corresponding to the MOD of 29 machines group, also converges to the same UEP with 29 generators advanced.

Upon verifying this inter-area mode type of UEP solution, the following results were obtained. The inter-area mode of system separation is caused by the heavily loaded BRUCE units in the transmission-limited, post-disturbance network. To conduct the UEP verification test developed in Chapter V, the BRUCE generation is perturbed and the corresponding change in the post-disturbance equilibrium is observed. The ΔP_m was applied at the BRUCE machines 9

and 25:

1) UEP list = [1-17, 19, 20-27, 33-35].

2) $\Delta\underline{\theta}^{s2}$ sorted list = [25, 9, 15, 14, 21, 22, 16, 27, 19, 6, 17, 12, 20, 26, 8, 3, 24, 5, 4, 13, 2, 23, 35, 7, 10, 1, 33, 34, 11].

A comparison of these lists showed that the first 29 M/C in the $\Delta\underline{\theta}^{s2}$ sorted list were all contained in the UEP list validating the UEP.

Table 7.11 shows the typical stability assessment of interest in this NANTICOKE case. The stability limit is obtained in terms of total generation of NANTICOKE machines 20 and 26. Table 7.11 demonstrates how the normalized energy margin can be useful in the calculation of stability limits. The approximate stability limit computed in the table is 3803 MW. The stability limit obtained in time simulation is 3935 MW.

The results of Table 7.11 demonstrate the potential use of the TEF method for fast computation of the stability limits, within a reasonable accuracy.

The UEP verification test was applied to several inter-area mode cases. These results are briefly summarized below. NANTICOKE 3950 MW case with the fault at MILTON 500 kv bus: The same 50-generator NANTICOKE system, with the three-phase fault at the MILTON 500 kv bus was observed again to be an inter-area mode case. The MOD selected (Table 7.6) consists of 16 generators. The ray point corresponding to this MOD converged to a UEP with 29 generators advanced (same group of 29 M/C discussed in the earlier verification test). The ΔP_m was applied

Table 7.11. OH 50-generator system, NANTICOKE case - stability assessment

	NANTICOKE 3700 MW	NANTICOKE 3950 MW
ΔV_{PE}	9.094	3.868
$V_{KE_{(corr)}}$ at $t_{c\ell}$	6.493	7.625
$\Delta V_{PE}\|_n$	1.401	0.507
ΔV = energy margin	2.345	-3.757
Normalized energy margin ($\Delta V\|_n$)	0.347	-0.493
Remarks	stable	unstable
Approximate stability limit of NANTICOKE generation using linear interpolation between $\Delta V\|_n$ values	3803 MW	

at the BRUCE machines, which primarily caused the stressed conditions. The UEP list and $\Delta\underline{\theta}^{s2}$ list agreed with each other.

115-generator OH system

The inter-area mode type of UEP solution was obtained in this case while attempting to compute the stability limit for BRUCE generation. In this case, there were six BRUCE machines that were heavily loaded and responsible for the stress. The NANTICOKE generation was only 2500 MW. The BRUCE generation was 4800 MW. The details of the disturbance and the MOD selected are provided in Table 7.7. The ray point corresponding to 19 M/C advanced (MOD selected) starting point, converged to the UEP with 57 machines advanced. The ΔP_m was applied at the BRUCE machines. The UEP verification test was performed. The $\Delta\underline{\theta}^{s2}$ sorted list correctly identified the 57 machines that were found advanced in the UEP solution.

Justification when no UEP solution is obtained

In the cases of heavy loading of the system combined with extreme inadequacies in the transmission, the post-disturbance system was found to be steady-state unstable. In such situations, the UEP solution could not be obtained, as in the case of OH 100-generator system (MANITOBA case, for a three-phase fault at KENORA). Upon examination, it was revealed that the so-called stable equilibrium point of the system converged to was steady-state unstable to start with. The Lyapunov's indirect method and the computation of synchronizing coefficients, discussed in Chapter V, confirmed the

steady-state instability. In such cases, the transient stability assessment will not be performed.

Discussions

1) It is apparent that the transient stability analysis of stressed systems must include verifiying whether the post-disturbance system is steady-state stable if no UEP solution is obtained.

2) Owing to the severe numerical ill-conditioning caused by the stress, the poor selection of UEP solution technique may lead to divergence in UEP solution, and subsequently, an erroneous stability assessment. It is important to apply the UEP verification test when the inter-area mode type of UEP solution is obtained.

CHAPTER VIII. SUMMARY AND CONCLUSIONS

This investigation of applying the transient energy function (TEF) method to stressed large-scale power systems mainly involved the following three phases:

1) Understanding the complex transient behavior of the stressed systems and identifying the key parameters of the system that primarily cause system separation, when it occurs.

2) Dealing with the analytical and numerical problems encountered, when the TEF method is used to study the complex instability phenomena of stressed systems.

3) Validating and verifying the new developments for reliability and efficiency of the stability assessment in stressed systems.

From the data provided, the following comments on the transient behavior of the stressed systems can be made:

- For a given network with transmission limitations, the stressed conditions occur, when the heavy loading of certain critical power plants is associated with heavy power flows on these transmission lines.
- The dominant transient behavior may not be that of the inertial response of the machines that are electrically close to the disturbance. Rather, it may be that of a large group of generators with respect to the rest of the system.

  This is in sharp contrast to the well-studied behavior of the unstressed systems of study with the TEF method, often found in the literature.

- Thus, when the disturbance is severe enough, the so-called inter-area mode of separation occurs. The effect of stress (large impedances and heavy generation) contributes to weak synchronizing forces between the large group of generators, and the rest of the generators. This leads to the final dominance of the inter-area mode of oscillation.

The following developments and enhancements were made to extend the application of the TEF method to stressed large-scale power systems:

1) Automatic determination of the mode of disturbance (MOD) to identify and characterize the controlling unstable equilibrium point (UEP) for a given disturbance under investigation.

2) Corrected-Gauss-Newton (CGN) method, a robust and reliable algorithm, tailored for UEP solutions under stressed system conditions. Obtaining a reliable and efficient starting point to converge to the UEP of interest.

3) Verifying the UEP solution obtained, wherever the shift in the mode of disturbance is encountered. Justifying the absence of UEP by verifying the post-disturbance system to be steady-state unstable.

These new developments were tested on two realistic power networks derived from the large base case of the Ontario Hydro system. The initial and post-disturbance conditions selected for the study represent highly stressed power system conditions. The test networks included two unstressed systems, for the sake of documenting the overall performance of TEF method with its new developments. From the results, the following conclusions were drawn:

- The scheme for MOD determination accurately predicts the MOD in the controlling UEP for the cases where the inter-area mode is not dominant. In the cases involving inter-area mode, MOD predicted is the group of generators most severely disturbed initially. However, it provided satisfactory bounds on the controlling UEP in terms of reliable convergence. In such situations, the UEP verification test confirmed that the shift in MOD, late in the transient, is justifiable.
- The MOD predicted is the most severely disturbed group of generators following the disturbance. This group of generators determines the kinetic energy that tends to split the system at the end of the disturbance period into two groups pulling away from each other.
- Based on the studies made, the inter-area mode of system separation is explained as the following. Due to the weak synchronizing forces which exist in the system, some other generators away from the disturbance are also affected in a slowly developing transient. As a result, the generators predicted in the MOD test cannot lose synchronism without the other generators also separating.
- The UEP solution reflected the inter-area mode of separation accurately and was in agreement with the results obtained by conventional time simulation.
- The CGN method - UEP solution technique was found to be extremely reliable in dealing with the severe numerical ill-conditioning encountered in stressed systems.

- In the cases involving the inter-area mode dominance, the UEP verification test is found to be essential, since the numerical techniques are very vulnerable to divergence. This test provides a systematic way to verify the shift in MOD observed in the UEP solution.
- The absence of UEP solution and the associated steady-state instability of the post-disturbance system illustrates the extreme effects of stress.
- The overall performance of the TEF method, with regard to the transient stability assessment in stressed system (stability or instability and stability limits of critical plant generation), was found to be reasonably accurate in agreement with the conventional time simulations.

Suggestions for Future Research

Based on the experience in the present investigation, the following developments are recommended:

- The scheme for determination of the mode of disturbance (MOD) makes an engineering assumption to select different groupings of generators from the list of key machines obtained. This issue was presented in the discussions in Chapter VII, following the results of the MOD predictions.

  Further effort is recommended in identifying the circumstances, if any, where this assumption requires improvement.

- Proper application of the UEP verification test relies on the analyst's implicit knowledge of the heavily loaded machines in the system that primarily cause the inter-area mode of system separation.

  Additional effort is recommended toward a systematic way of identifying these heavily loaded machines in the post-disturbance system. This may enable the method to be extended to an on-line environment of stability analysis in power system operation.

- The application of the TEF method to ill-conditioned, very large networks (over 150 generators) may need further improvements with regard to the speed of the CGN method in UEP solutions. .

The following additional suggestions may be worth investigating, in extending the TEF method to practical, realistic stability studies.

1) Sparse formulation, preserving the structure of the network, may be attempted for the following reasons:

- Avoiding the round-off error introduced by the network reduction, in the present reduced system formulation. (The numerical ill-conditioning of the stressed system may be aggravated by these errors.)
- To enable the future problem formulations, such as the provisions for nonlinear load modeling and the study of voltage instability at key load busses.

2) The inter-area mode of system separation is found to be a slowly developing transient. The effect of very fast exciters may preferably be included to obtain more accurate computations of stability limits in the operation of the stressed systems.

BIBLIOGRAPHY

1. IEEE Committee Report. "Proposed Terms and Definitions for Power System Stability." IEEE Trans. PAS-101 (1982): 1894-1898.

2. El-Kady, M. A., Tang, C. K., Carvalho, V. F., Fouad, A. A. and Vittal, V. "Dynamic Security Assessment Utilizing the Transient Energy Function Method." Proc. of the 1985 PICA Conference, San Francisco, California, May 1985.

3. IEEE Committee Report, Anjan Bose, Chairman. "Application of Direct Methods to Transient Stability Analysis of Power Systems." IEEE Trans. PAS-103 (July 1984): 1628-1636.

4. "Network Access and the Future of Power Transmission." EPRI Journal 11 (April 1986): 4-13.

5. Young, C. C. "Analytical Needs in the Western Area." Proc. of the International Symposium on Power System Stability, Ames, Iowa, May 1985.

6. Anderson, P. M. and Fouad, A. A. Power System Control and Stability. Vol. 1. Ames, Iowa: Iowa State University Press, 1977.

7. Athay, T., Sherket, V. R., Podmore, R., Virmani, S. and Puech, C. "Transient Energy Analysis." Proc. of the Conference on Systems Engineering for Power: Emergency Operating State Control, Davos, Switzerland, 1979.

8. Fouad, A. A., Kruempel, K. C., Mamandur, K. R. C., Pai, M. A., Stonton, S. E. and Vittal, V. "Transient Stability Margin as a Tool for Dynamic Security Assessment." EPRI Report EL-1755, March 1981.

9. Fouad, A. A., Vittal, V. and Oh, Takeyoo. "Critical Energy for Transient Stability Assessment of a Multimachine Power System." IEEE Trans. PAS-103 (1984): 2199-2206.

10. Aylett, P. D. "Energy-Integral Criterion of Transient Stability Limits of Power Systems." Proc. of IEE 105[C] (July 1958): 527-536.

11. Lugtu, R. L. and Fouad, A. A. "Transient Stability Analysis of Power Systems Using Lyapunov's Second Method." IEEE Winter Meeting, Paper No. C72145-6, New York, February 1972.

12. Tavora, C. J. and Smith, O. J. M. "Characterization of Equilibrium and Stability in Power Systems." IEEE Trans. PAS-91 (May 1972): 1127-1130.

13. Gupta, C. L. and El-Abiad, A. H. "Determination of the Closest Unstable Equilibrium State for Lyapunov Methods in Transient Stability Studies." IEEE Trans. PAS-94 (September 1976): 1699-1712.

14. Kakimato, N., Ohsawa, Y. and Hayashi, M. "Transient Stability Analysis of Electric Power Systems via Lure Type Lyapunov Function." Proceedings of IEE Japan 98 (May/June 1978): 63-78.

15. Ribbens-Pavella, M., Grujic, L. T., Sabatel, J. and Bouffioux, A. "Direct Methods for Stability Analysis of Large-Scale Power Systems." Proc. of the IFAC Symposium on Computer Applications in Large-Scale Power Systems, New Delhi, India, August 1979, Pergamon Press, U.K.

16. Uyemura, K. and Matsuki, J. "Computational Algorithms for Evaluating Unstable Equilibrium States in Power Systems." Electrical Engineering in Japan 92 (July/August 1972): 41-47.

17. Bergen, A. R. and Hill, D. J. "A Structure Preserving Model for Power System Stability Analysis." IEEE Trans. PAS-100 (January 1981): 25-35.

18. Fouad, A. A. and Stanton, S. E. "Transient Stability of Multi-machine Power Systems, Parts I and II." IEEE Trans. PAS-100 (July 1981): 3408-3424.

19. Fouad, A. A. and Vittal, V. "Power System Response to a Large Disturbance: Energy Associated with System Separation." Proc. of the 1983 PICA Conference, Houston, TX, May 1983.

20. Michel, A. N., Fouad, A. A. and Vittal, V. "Power System Transient Stability Analysis Using the Individual Machine Energy Functions." IEEE Trans. on Circuits and Systems (CAS) 30 [5] (May 1983): 266-276.

21. Miller, R. K. and Michel, A. N. Ordinary Differential Equations. New York: Academic Press, 1982.

22. Fouad, A. A., Kruempel, K. C., Vittal, V., Ghafurian, A., Nodehi, K. and Mitsche, J. V. "Transient Stability Program Output Analysis." IEEE Trans. PWRS-1 (February 1986): 2-9.

23. Ribbens-Pavella, M., Lemal, B. and Pirard, W. "On-line Operation of Lyapunov Criterion for Transient Stability Studies." Proc. IFAC Symposium, Melbourne, Australia, 1977.

24. Pai, M. A. Power System Stability Analysis by the Direct Method of Lyapunov. Volume 3. New York: North-Holland Systems and Control Series, 1981.

25. Gill, P. E., Murray, W. and Wright, M. H. Practical Optimization. New York: Academic Press, 1981.

26. Schwefel, H. Numerical Optimization of Computer Models. New York: John Wiley & Sons, 1981.

27. El-Abiad, A. H. and Nagappan, K. "Transient Stability Regions of Multi-machine Power Systmes." IEEE Trans. PAS-85(2) (February 1966): 169-178.

28. Gill, P. E. and Murray, W. "Algorithms for the Solution of the Nonlinear Least-Squares Problem." Am. J. Numer. Anal. 15(5) (October 1978): 977-992.

29. Vidyasagar, M. Nonlinear Systems Analysis. Englewood Cliffs, New Yersey: Prentice-Hall, 1978.

30. Vittal, V., Rajagopal, S., McCormack, B. C., Movall, P. E. and Fouad, A. A. "Analysis of Potential Energy Surfaces of Multimachine Power Systems Using Computer Graphics." IEEE Trans. on Education E-20, No. 4 (November 1986): 181-185.

ACKNOWLEDGMENTS

I would like to thank my major professors, Dr. A. A. Fouad and Dr. V. Vittal, for their invaluable guidance and attention throughout this work. Their professional enthusiasm motivated me to overcome the occasional setbacks during the course of this research endeavor. In particular, I am extremely thankful for the time they spent in the numerous discussions. It gave me a unique opportunity to develop my analytical skills.

I am thankful to Dr. K. C. Kruempel, who exposed me, during my graduate program, to the special computer programming skills required for power systems analysis. Special thanks are extended to Professor R. G. Brown for his participation in my Program of Study Committee. I would like to thank Professor R. J. Lambert for his enthusiastic participation in my graduate committee.

I am indebted to the Department of Electrical Engineering at Iowa State University for their financial support during my graduate program.

I sincerely appreciate Dr. M. A. El-Kady and Dr. V. F. Carvalho of the Ontario Hydro for providing me with the valuable data to conduct this investigation. I thank them once again for their comments and suggestions during this work.

I would like to thank my parents for their moral support and encouragement throughout my graduate program.

Special thanks are extended to Ms. Barbara Dubberke for her excellent typing of this dissertation and her cooperation.

APPENDIX A: COMPUTER PROGRAMS DEVELOPED

Computer Program 'MOD'

The procedure provided in Chapter III for the automatic determination of the mode of disturbance was programmed as FORTRAN source code 'MOD'. Figure A.1 explains the flow chart of 'MOD'.

The output listing of the program mainly includes the following information:

- list of key machines
- candidate groupings and their corresponding $KE_{(corr)}$ values
- selected candidate groupings for ray point computation and their corresponding $\Delta V_{PE}|_n$
- ray point corresponding to the MOD predicted, to be used as the starting point for the UEP solution.

Computer Program 'CGN'

The algorithm of the corrected-Gauss-Newton method is furnished in Chapter IV. The program layout of the FORTRAN source code 'CGN' is shown in Figure A.2. The details of each block of this figure are briefly explained in Table A.1.

The output listing of the program mainly consists of the following information:

- starting value $\underline{\theta}$, rotor angles
- mismatch function vector
- objective function and its gradients

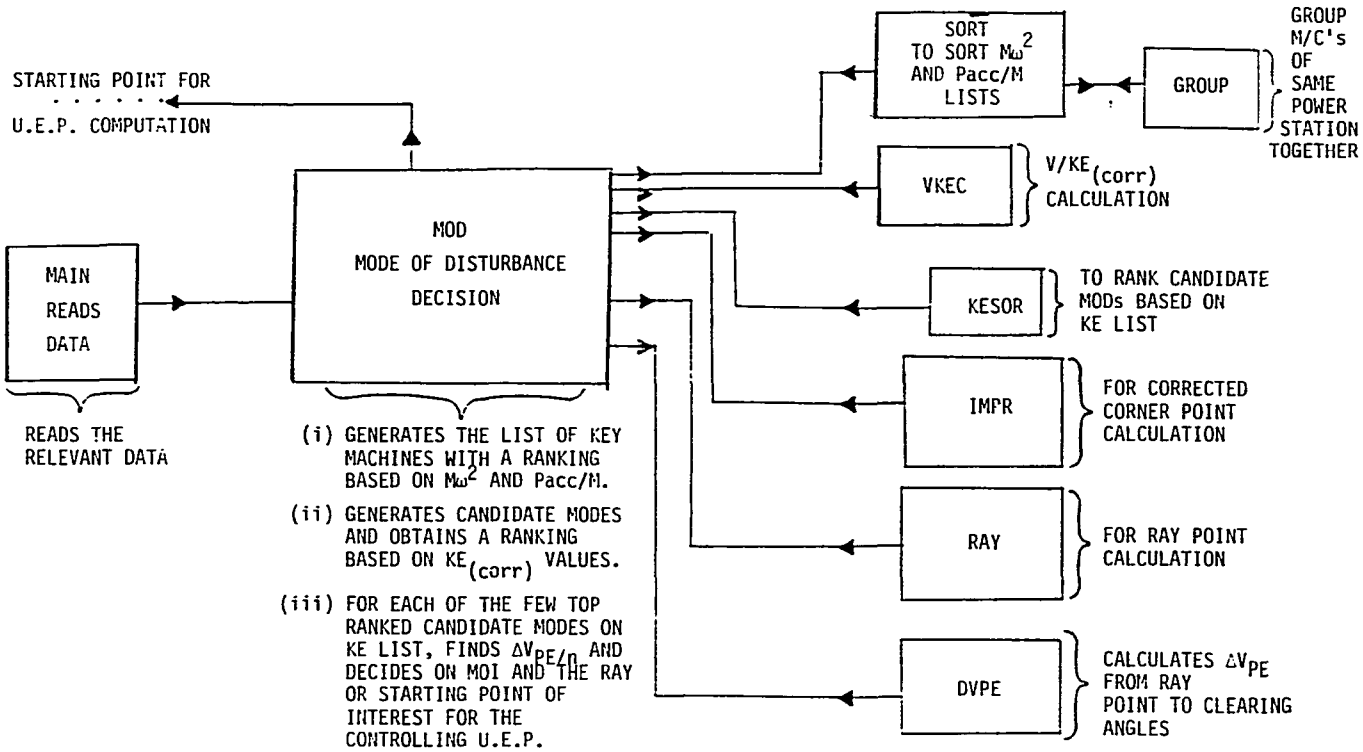

Figure A.1. Flow chart of 'MOD'

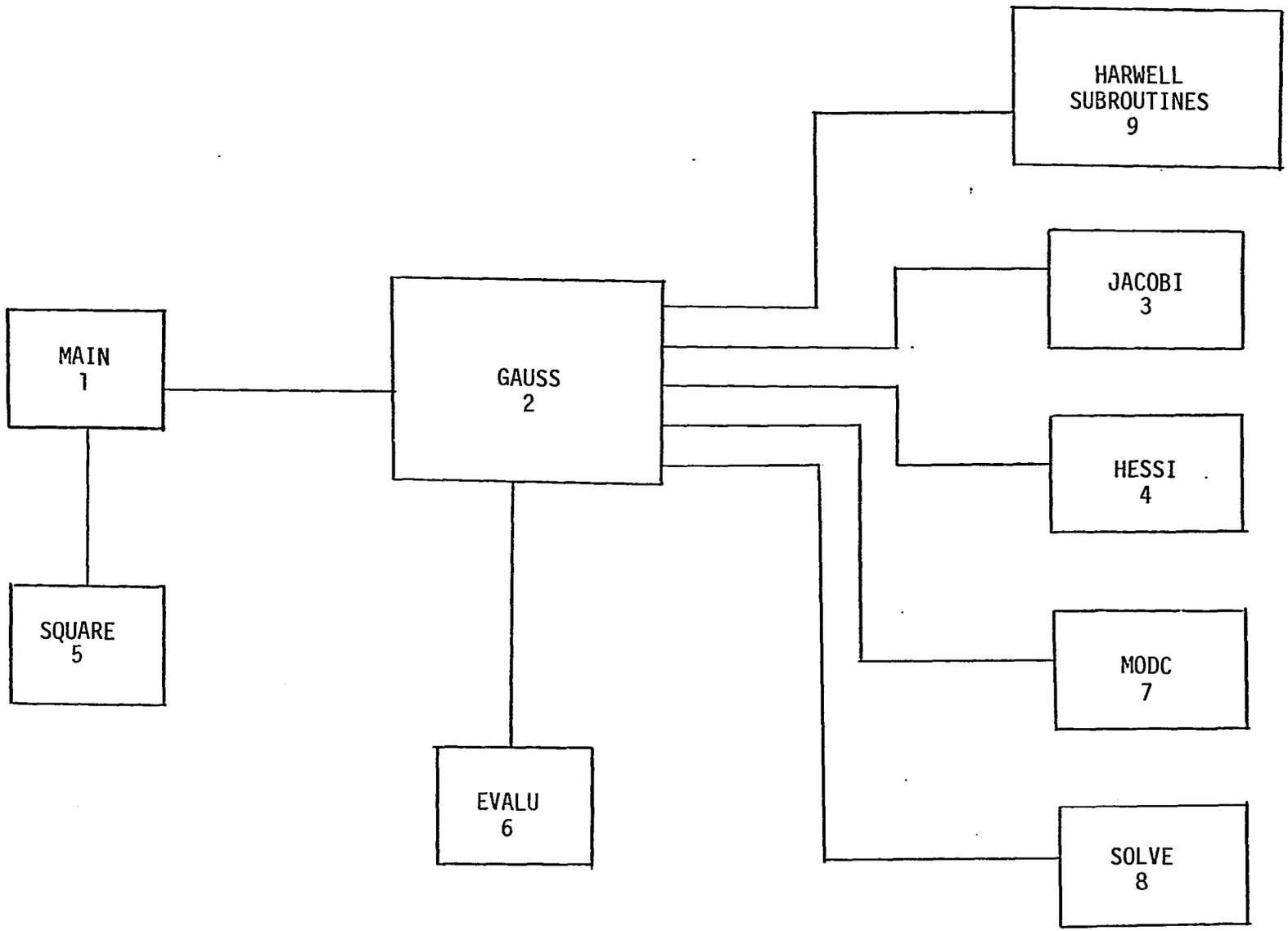

Figure A.2. 'CGN' program layout

Table A.1. Explanation of 'CGN' layout

No.	Name	Purpose
1	MAIN	Reading data and arranging data for computing an equilibrium point.
2	GAUSS	Algorithm of Gill and Murray [28] for Corrected-Gauss-Newton method.
3	JACOBI	Computes Jacobian $[\frac{\partial f_i}{\partial \theta_j}]$ (N X N-1) matrix; gradient $[\frac{\partial (FBIG)}{\partial \theta_i}]$ N-1 X 1 vector and FBIG = $\sum_{i=1}^{n} f_i^2$.
4	HESSI	Computes second differential information required for correction steps. B matrix = $\sum_{k=1}^{n} f_k [\frac{\partial f_k}{\partial \theta_i \partial \theta_j}] = \sum_{k=1}^{n} f_k$ [Hessian of f_k] (size N-1 X N-1). Normally, 'HESSI' is called in case of stressed and ill-conditioned systems of study.
5	SQUARE	Computes a N X N square Jacobian matrix, if necessary, for eigenvalue analysis for checking steady-state stability.
6	EVALU	Evaluates the quality of local minimum; if $\|\|J^T J\\|$ > > FBIG, at the time algorithm stops, the solution is a valid local minimum.

Table A.1. Continued

No.	Name	Purpose
7 8	MODC SOLVE	Modified Cholesky factorization and corresponding solution required for correction steps. If $\underline{A}$ is ill-conditioned, finds a correction $\underline{E}$ to form $\hat{\underline{A}} = \underline{A} + \underline{E} = \underline{L}\,\underline{D}\,\underline{L}^T$ in order to find an approximate solution to $\underline{X}$ in $\hat{\underline{A}}\,\underline{X} \cong \underline{A}\,\underline{X} = \underline{B}$.
9	HARWELL SUBROUTINES	Subroutines EB10A, FM01AS, FM07A, MC25A and MC26A for singular value decomposition.

- singular values of Jacobian
- direction of search (Gauss-Newton step and correction step, if necessary)
- updated value of $\underline{\theta}$ in each iteration performed and the final UEP solution obtained.

APPENDIX B: EXPRESSIONS FOR FIRST AND SECOND DERIVATIVES IN 'CGN'

The mismatch function vector $\underline{f}$ in the right-hand side of the swing equation defined in Eqs. (2.6) and (4.5), reproduced as the following:

$$f_i(\underline{\theta}) = P_i - P_{ei} - \frac{M_i}{M_T} P_{COI} \triangleq f_i \tag{B.1}$$

where θ_i is the rotor angle, the variable of interest for a machine i in a n-machine system and

$$P_{ei} = \sum_{\substack{j=1 \\ j\neq i}}^{n} D_{ij}\cos\theta_{ij} + C_{ij}\sin\theta_{ij} \tag{B.2}$$

where the constants C_{ij}, D_{ij}, M_i, M_T and P_i are defined in Eq. (2.2), $\theta_{ij} \triangleq \theta_i - \theta_j$ and

$$P_{COI} = \sum_{i=1}^{n} P_i - P_{ei} = \sum_{i=1}^{n} P_i - 2 \sum_{i=1}^{n-1} \sum_{j=i+1}^{n} D_{ij}\cos\theta_{ij} \quad . \tag{B.3}$$

The objective function is defined as

$$F(\underline{\theta}) = \sum_{i=1}^{n} f_i^2 \triangleq F \quad . \tag{B.4}$$

Due to the inertial center reference frame (COI reference), θ_1 to θ_{n-1} are considered as independent variables and θ_n is the dependent variable of the machine with the largest inertia. θ_n will be a linear combination of θ_1 to θ_{n-1}, i.e.,

$$\theta_n = - \sum_{i=1}^{n-1} \frac{M_i \theta_i}{M_n} \quad .$$

The Jacobian of $\underline{f}$ is defined as the matrix $[J_{ij}]$,

$$\underline{J} = [\frac{\partial f_i}{\partial \theta_j}] \qquad i = 1, n; \; j = 1, n-1 \quad . \tag{B.5}$$

The gradient of F is defined as the vector (g_i),

$$\underline{g} = (\frac{\partial F}{\partial \theta_i}) \qquad i = 1, n-1$$

$$= 2 \, \underline{J}^T \underline{f} \quad . \tag{B.6}$$

The Hessian of f_i is defined as the matrix $\underline{G}_i$ for every ith machine:

$$\underline{G}_i = [\frac{\partial f_i}{\partial \theta_j \, \partial \theta_k}] \qquad j = 1, n-1; \; k = 1, n-1 \text{ for a given } i. \tag{B.7}$$

The matrix $\underline{B}$ is defined as

$$\underline{B} = \sum_{i=1}^{n} f_i \, \underline{G}_i \quad . \tag{B.8}$$

The explicit computation is required for the Jacobian $\underline{J}$ in all iterations and $\underline{G}_i$, i=1, n-1, the Hessian matrices only for the iterations involving correction steps (taken in the case of numerical ill-condition). From $\underline{J}$ and $\underline{G}_i$, the gradient $\underline{g}$ and matrix $\underline{B}$ can be

calculated directly as shown in Eqs. (B.6) and (B.8).

The (i,j) element of the Jacobian matrix, J_{ij}, is calculated explicitly as

$$J_{ij} = \frac{\partial f_i}{\partial \theta_j} = - \frac{\partial P_{ei}}{\partial \theta_j} - \frac{M_i}{M_T} \frac{\partial P_{COI}}{\partial \theta_j} \qquad \text{(B.9)}$$

$$i = 1, n \text{ and } j = 1, n-1 \ .$$

The (i,j) element of the Hessian $\underline{G}_k$ is defined as

$$G_{k_{i,j}} = - \frac{\partial^2 P_{ek}}{\partial \theta_i \, \partial \theta_j} - \frac{M_i}{M_T} \frac{\partial^2 P_{COI}}{\partial \theta_i \, \partial \theta_j} \qquad \text{(B.10)}$$

$$i = 1, n-1 \text{ and } j = 1, n-1$$

$$\text{for a given } k = 1, n \ .$$

Thus, the first derivatives computed in the closed form are the $\partial P_{ei}/\partial \theta_j$, $\partial P_{COI}/\partial \theta_j$ terms in Eq. (B.9). The second derivatives computed in the closed form are the $\partial^2 P_{ek}/\partial \theta_i \, \partial \theta_j$, $\partial^2 P_{COI}/\partial \theta_i \, \partial \theta_j$ terms in Eq. (B.10).

The first derivatives to be computed are:

$$\text{define} \qquad d(\theta_i, \theta_j) \stackrel{\Delta}{=} - D_{ij} \sin\theta_{ij} + C_{ij} \cos\theta_{ij} \qquad \text{(B.11)}$$

$$\frac{\partial P_{ei}}{\partial \theta_i} = \sum_{\substack{j=1 \\ j\neq i}}^{n-1} d(\theta_i, \theta_j) + d(\theta_i, \theta_n)\left(1 + \frac{M_i}{M_n}\right)$$

$i=1, n-1$

$$\frac{\partial P_{ei}}{\partial \theta_j} = -d(\theta_i, \theta_j) + d(\theta_i, \theta_n)\frac{M_j}{M_n}$$

$i\neq j \quad i,j=1, n-1$

and

$$\frac{\partial P_{en}}{\partial \theta_i} = \sum_{\substack{j=1 \\ j\neq i}}^{n-1} -d(\theta_n, \theta_j)\frac{M_i}{M_n} - d(\theta_n, \theta_i)\cdot\left(1 + \frac{M_i}{M_n}\right)$$

$i=1, n-1$ (B.12)

$$\frac{\partial P_{COI}}{\partial \theta_i} = 2\left[\sum_{\substack{j=1 \\ j\neq i}}^{n-1} D_{ij}\sin\theta_{ij} + \sum_{\substack{j=1 \\ j\neq i}}^{n-1} D_{jn}\sin\theta_{jn}\frac{M_i}{M_n} + D_{in}\sin\theta_{in}\left(1 + \frac{M_i}{M_n}\right)\right]$$

$i=1, n-1$ (B.13)

The second derivatives computed are:

$$\text{define} \quad e(\theta_i, \theta_j) = -D_{ij}\cos\theta_{ij} - C_{ij}\sin\theta_{ij} \tag{B.14}$$

$$\frac{\partial^2 P_{ei}}{\partial\theta_i\,\partial\theta_i} = \sum_{\substack{j=1\\ j\neq i}}^{n-1} e(\theta_i, \theta_j) + e(\theta_i, \theta_n)\cdot\left(1+\frac{M_i}{M_n}\right)^2$$

$i=1, n-1$

$$\frac{\partial^2 P_{ei}}{\partial\theta_i\,\partial\theta_j} = -e(\theta_i, \theta_j) + e(\theta_i, \theta_n)\cdot\left(1+\frac{M_i}{M_n}\right)\frac{M_j}{M_n}$$

$i,j=1, n-1$
$i\neq j$

$$\frac{\partial^2 P_{ek}}{\partial\theta_i\,\partial\theta_i} = e(\theta_k, \theta_i) + e(\theta_k, \theta_n)\left(\frac{M_i}{M_n}\right)$$

$k\neq i,\ k,i=1, n-1$

$$\frac{\partial^2 P_{ek}}{\partial\theta_i\,\partial\theta_j} = e(\theta_k, \theta_n)\frac{M_i}{M_n}\cdot\frac{M_j}{M_n}$$

$k\neq i,j$
$i\neq j$ $\quad k,i,j=1, n-1$

$$\frac{\partial^2 P_{en}}{\partial\theta_i\,\partial\theta_i} = \sum_{\substack{j=1\\ j\neq i}}^{n-1} d(\theta_n, \theta_j)\left(\frac{M_i}{M_n}\right)^2 + e(\theta_n, \theta_i)\left(1+\frac{M_i}{M_n}\right)^2$$

$i=1, n-1$

$$\frac{\partial^2 P_{en}}{\partial\theta_i\,\partial\theta_j} = \sum_{\substack{k=1\\k\neq i,j}}^{n-1} e(\theta_n, \theta_k)\,\frac{M_i}{M_n}\cdot\frac{M_j}{M_n}$$

$i\neq j,\ i,j=1,\ n-1$

$$+ e(\theta_n, \theta_i)\,\left(1 + \frac{M_i}{M_n}\right)\cdot\frac{M_j}{M_n}$$

$$+ e(\theta_n, \theta_j)\,\left(1 + \frac{M_j}{M_n}\right)\cdot\frac{M_i}{M_n} \qquad \text{(B.15)}$$

$$\frac{\partial^2 P_{COI}}{\partial\theta_i\,\partial\theta_i} = 2\left[\sum_{\substack{j=1\\j\neq i}}^{n-1} D_{ij}\cos\theta_{ij} + \sum_{\substack{j=1\\j\neq i}}^{n-1} D_{jn}\cos\theta_{jn}\left(\frac{M_i}{M_n}\right)^2 + D_{in}\cos\theta_{in}\left(1 + \frac{M_i}{M_n}\right)^2\right]$$

$i=1,\ n-1$

$$\frac{\partial^2 P_{COI}}{\partial\theta_i\,\partial\theta_j} = 2\left[-D_{ij}\cos\theta_{ij} + \sum_{\substack{k=1\\k\neq i,j}}^{n-1} D_{kn}\cos\theta_{kn}\cdot\frac{M_i}{M_n}\cdot\frac{M_j}{M_n}\right.$$

$i\neq j,\ i,j=1,\ n-1$

$$+ D_{in}\cos\theta_{in}\left(1 + \frac{M_i}{M_n}\right)\cdot\left(\frac{M_j}{M_n}\right)$$

$$\left. + D_{jn}\cos\theta_{jn}\left(1 + \frac{M_j}{M_n}\right)\cdot\frac{M_i}{M_n}\right] . \qquad \text{(B.16)}$$